

Mapping spatial variability of the frequency-magnitude distribution of earthquakes

Stefan Wiemer¹ and Max Wyss²

¹Institute of Geophysics; ETH Hoenggerberg; CH-8093; Zurich, Switzerland; tel. +41 633 6625; fax 1065; stefan@seismo.ifg.ethz.ch.

²Geophysical Institute; University of Alaska Fairbanks; AK 99775-7320; USA; max@giseis.alaska.edu.

Advances in Geophysics, in press.

Abstract

Mapping the earthquake-size distribution in various tectonic regimes on a local to regional scale reveals statistically significant variations in the range of at least 0.4 to 2.0 for the b -value in the frequency-magnitude distribution. With the computer program ZMAP, these changes can be mapped in detail in two and three dimensions, and temporal changes of b can be mapped quantitatively. The five new hypotheses we propose are the following. (1) Active magma chambers in seismogenic crust may be mapped by an excess of small earthquakes, which can be measured by anomalously large b -values. (2) Fault asperities may be mapped by maxima in local earthquake probability (minima in local recurrence time). (3) Permanent changes in the probability for earthquakes, caused by major and large shocks in their vicinity, can be estimated from the changes in local recurrence time, calculated from changes in a - and b -values. (4) Dehydration, and thus the deep source of magma for subduction volcanism, may be mapped by anomalously high b -values in deep seismic zones. (5) The b -values in aftershock sequences are heterogeneous, suggesting that the probability of a major aftershock varies in space. In this paper, we review case studies pertaining to these hypotheses. The strongest variations are found in nine volcanic regions studied so far, where small volumes ($r = 1.5$ km) of b -values larger than 1.3 are embedded in normal crust ($b \leq 1$). High b -value anomalies are also found at the top of the subducting slabs in Alaska, New Zealand and Japan,

at depths of 100 – 150 km, possibly indicating regions of dehydration-introduced melting. Asperities, or strong patches of faults, on the other hand seem to be characterized by low b -values ($b < 0.6$) in volumes with radii ranging from 5 to 40 km, along the San Andreas fault in central and southern California, in Japan and Mexico. In aftershock zones, we find the lowest b -values outside the main shock rupture areas. The differences in b - and a -values observed in aftershock sequences, as well as during many years after main shocks in their vicinity, allow us to calculate and map changes in the local probability of earthquakes as a function of space and time. These changes are substantial and may be useful for refining the earthquake hazard assessment. Our results suggest that detailed mapping of the frequency-magnitude distribution on a local to regional scale is an effective tool for the investigation of several aspects of seismically active zones.

1. Introduction

The size distribution of earthquakes in a seismogenic volume can often be adequately described over a large range of magnitudes [Abercrombie, 1995] by a power law relationship. This was first recognized in Japan by *Ishimoto and Iida* [1939] and in California by *Gutenberg and Richter* [1944]. The commonly used form of the power law is given as

$$\log N = a - b M \quad (1)$$

where N is the cumulative number of earthquakes with magnitude $\geq M$, and a and b are constants. The parameter ‘ a ’ describes the productivity of a volume, and b , the slope of the frequency-magnitude distribution (FMD), describes the relative size distribution of events. The example in Figure 1 shows the FMD for southern California for the years 1995 - 2000. The b -value equals 0.99, and $a=6.08$.

The numerous papers that have been written about the FMD, specifically the b -value, fall into several categories:

- 1) Studies addressing how the b -value and its uncertainty is computed accurately [*Aki*, 1965; *Bender*, 1983; *Hamilton*, 1967; *Page*, 1968; *Shi and Bolt*, 1982; *Utsu*, 1965; *Utsu*, 1992; *Utsu*, 1999; *Zuniga and Wyss*, 1995; *Gibowicz and Lasocki*, 2001; *Kijko and Sellevoll*, 1989; *Tinti*, 1989; *Tinti and Mulargia*, 1987].
- 2) Studies addressing temporal variations of b , some of them relating to earthquake prediction [*Patane et al.*, 1992; *Wiemer and Benoit*, 1996; *Wiemer and McNutt*, 1997; *Wiemer and Wyss*, 1997; *Wiemer and Katsumata*, 1999; *Wyss and Lee*, 1973; *Wyss et al.*, 1997; *Wyss et al.*, 2000; *Zobin*, 1979].

- 3) Studies addressing the shape of the FMD for the largest magnitudes, and the implication for hazard [*Abercrombie and Brune*, 1994; *Kagan*, 1999; *Main*, 2000; *Pacheco et al.*, 1992; *Schwartz and Coppersmith*, 1984; *Stein and Hanks*, 1998; *Utsu*, 1999; *Wesnousky*, 1994].
- 4) Studies relating b -values to physical properties such as stress, material homogeneity and pore pressure [*Lockner and Byrlee*, 1991; *Mogi*, 1962; *Scholz*, 1968; *Shaw*, 1995; *Warren and Latham*, 1970; *Wyss*, 1973].
- 5) Studies investigating implications of the power law scaling in light of the concepts of fractal dimension and chaotic behavior [*Amelung and King*, 1997; *Bak and Tang*, 1989; *Barton et al.*, 1998; *Henderson et al.*, 1992; *Hirata*, 1989; *Ito and Matsuzaki*, 1990; *Main*, 1995; *Main*, 1996; *Sammis et al.*, 2001; *Okuda et al.*, 1992; *Papadopoulos et al.*, 1993].
- 6) Studies addressing the spatial variability of b , from scales of mm in the laboratory to global scales [*Frohlich and Davis*, 1993; *Gerstenberger et al.*, 2001; *Imoto et al.*, 1990; *Jolly and McNutt*, 1999; *Mori and Abercrombie*, 1997; *Ogata et al.*, 1991; *Ogata and Katsura*, 1993; *Westerhaus et al.*, 2001; *Wiemer and Benoit*, 1996; *Wiemer and Wyss*, 1997; *Wiemer et al.*, 1998; *Wiemer and Katsumata*, 1999; *Wiemer et al.*, 2001; *Wyss et al.*, 2001ab; *Wyss and Wiemer*, 2000].

This paper addresses primarily point 6, spatial variability of b , on a local to regional scale (hundreds of meters to kilometers). It is not intended to be a comprehensive review of past work on b -values. We focus largely on our own recent results, since we are most familiar with them, and because we believe that our detailed mapping has opened some new directions of research, including previously unavailable information about properties of seismogenic volumes. In addition, topics such as temporal variations, fractal dimension and the correct estimate of b and its uncertainty will be discussed.

Spatially mapping b -values has proven a rich source of information about the seismotectonics of a region. The ample, high-quality earthquake catalogs collected primarily over the past two decades, and the availability of increased computing power, have enabled researchers to investigate spatial variations in b with an unprecedented level of detail. The notion that the earthquake size distribution can vary by up to a factor of three on a kilometer scale was first greeted with skepticism; however, with a growing number of case studies and rigorous statistical testing, acceptance is growing rapidly. In our understanding, the discovery of strong differences in b is simply a reflection of the heterogeneity of the earth that emerges on all scales, once suitable datasets become available. The first step in extracting information

from the heterogeneity in b -value is to determine with what other parameters these variations correlate.

We believe for two reasons that changes in the frequency-magnitude distribution as a function of time are generally more difficult to observe than spatial variations: (1) Network configuration and analyzing procedures are likely to change as a function of time and can introduce artifacts in the magnitudes reported [Habermann, 1987; Habermann, 1991; Wyss, 1991]. These changes in the reporting history can introduce artificial changes in the b -values, for example, a stretch in the frequency-magnitude distribution [Zuniga and Wyss, 1995]. (2) Temporal variations may often be second-order phenomena, compared with the first-order variations of the b value with location [1992; Wiemer and Wyss, 1997; Wiemer et al., 1998]. We have interpreted this as an indication that the production of earthquakes in a particular volume depends on stationary properties such as the crack distribution, and that a particular volume does not readily change the characteristics displayed. However, in volcanic systems and during large earthquakes, substantial changes in the crust do occur, such as the intrusion of a major dike or a change in pore pressure. We are particularly interested in comparing the pre-main shock and post-main shock b -values.

The purpose of this paper is to summarize the new facts surrounding the spatial variability of the b -value, to discuss the new hypotheses that grew from these observations, to report how far the tests of these hypotheses have advanced, and to describe the methods used, such that a reader can implement them.

2. Data Requirements

2.1 Estimating the magnitude of completeness

The correct estimate of the b - and a -values depends critically on the completeness of the sample under investigation. As seen in Figure 1, the FMD deviates from a linear power law fit increasingly for smaller magnitudes. This deviation is caused by the fact that the recording network is only capable of recording a fraction of all events for magnitudes smaller than the magnitude of completeness, M_c . Figure 2a shows the b -values as a function of M_c for a sample taken from the Parkfield region. An underestimate of M_c ($M_c < 1.2$) results in too low a b -value. For $1.2 < M_c < 2.2$, the estimate of b is about constant. If M_c is raised to large values, the uncertainty in the b -value estimate increases strongly (Figure 2a). At the same time, the resolution for mapping decreases. The situation is complicated by the fact that M_c varies as a function of space and time throughout all earthquake catalogs, hence estimating the correct M_c , while maximizing the available number of earthquakes, becomes difficult.

Different techniques can be used to estimate M_c [Gomberg, 1991; Kijko and Sellevoll, 1992; Rydelek and Sacks, 1989; Wiemer and Wyss, 2000]. A review with case studies is given by Wiemer and Wyss [2000]. A simple technique used frequently is based on estimating M_c from the FMD itself. This is often done in seismicity studies by visual examination of the cumulative or non-cumulative FMD; however, we prefer to apply a quantitative criterion [Wiemer and Wyss, 2000].

The following steps are taken to estimate M_c : First we estimate the b - and a -value of the FMD as a function of minimum magnitude, based on the events with $M \geq M_i$, using a maximum likelihood estimate [Aki, 1965; Bender, 1983; Shi and Bolt, 1982, see chapter 3.2]. Next, we compute a synthetic distribution of magnitudes with the same b -, a - and M_i values, which represents a perfect fit to a power law. To estimate the goodness of the fit, or percentage of data variability, we compute the absolute difference, R , of the number of events in each magnitude bin between the observed and synthetic distribution

$$R(a, b, M_i) = 100 - \left(\frac{\sum_i^{M_{\max}} |B_i - S_i|}{\sum_i B_i} \right) 100 \quad (2)$$

where B_i and S_i are the observed and predicted cumulative number of events in each magnitude bin. We divide by the total number of observed events to normalize the distribution. Our approach is illustrated in Figure 3, which shows R as function of M_i . If M_i is smaller than the 'correct' M_c the synthetic distribution based on a simple power law (squares in Figure 3) cannot model the FMD adequately and, consequently, the goodness of fit, measured in percent of the total number of events, is poor. The goodness of fit value R increases with increasing M_i , and reaches a maximum value of $R \sim 96\%$ at $M_c = 1.8$, in this example. At this M_c , a simple power law with the assumed b , a , and M_c can explain 96 percent of the data variability. Beyond $M_i = 1.8$, R increases again gradually. In this study, we map M_c at the 90% level, that is, we define M_c as the point at which a power law can model 90% or more of the FMD. For the example shown in Figure 3, we therefore define $M_c = 1.5$.

In some cases, the FMD cannot be approximated by a power-law [Knopoff, 2000; Pacheco et al., 1992; Trifu et al., 1995], because of bi-modal distributions (see also chapter 8.6). The estimation of M_c based on the power law assumption will generally break down in these locations. It is important to identify such regions when mapping b , because neither the M_c estimation is valid, nor does the b -value have the same meaning.

2.2 Trade off between spatial resolution and significance

To map the constants in the FMD in detail, we need as many events as possible, to be able to analyze small sub-volumes. The size of the volumes can also be reduced by limiting the numbers of events per sample. However, small sample sizes result in large uncertainties in the estimate of b . In Figure 2b, we show the results of a random simulation, based on a synthetic catalog of 5000 events with a b -value of 1.0. For sample sizes smaller than 50, the 5% and 95 % confidence regions are separated by more than 0.5 units, suggesting that only very large differences in b can be established with significance. For $N = 100$, this difference is about 0.25, and for $N = 200$ it is down to 0.2. Therefore, if the differences in b are large, samples of 50 events may be sufficient for statistical significance of the differences. If they are smaller, 1000 events per sample may be needed [Wyss and Wiemer, 2000b]. Thus, catalogs best suited for our analyses should cover long periods in highly seismic regions at small magnitudes of completeness. The smallest catalog we found useful for mapping likely magma chambers in a volume of about 10x10x20 km dimensions contained only 450 events [Murru *et al.*, 1999]; but mapping the change in earthquake probability in southern California due to the $M7.3$ Landers (1992) main shock required several 10s of thousands of events, because the temporal differences in b are small.

2.3 Maximizing the number of events

The longer the period included for analysis, the more earthquakes per volume become available, but, in general, the M_c is higher during early periods. When early parts of catalogs are used, the M_c for the entire data set must be raised, which reduces the number of events that may be included for recent periods. Often, this more than cancels the benefit of a long history. Thus, we usually maximize the number of events by selecting a starting time, t_s , that, together with the appropriate $M_c(t_s)$, leads to the maximum number of earthquakes in the catalog. In many parts of the United States and Japan that time is near 1980/1981. Because the t_s is selected on the basis of objective criteria, it is not a free parameter of the analysis.

2.4 Mapping minimum magnitude of completeness

The quality of all regional and local earthquake catalogs decreases from high at the center of the network, to low at the edges of the area monitored. Obvious boundaries of deterioration are coastlines, international borders and seams between networks. Offshore catalogs are generally higher in their level of M_c , but the homogeneity of reporting is better. This is true because the installation of more seismographs on land can change the M_c and the magnitude scale for events located beneath the landmass, but does not affect the reporting off shore. To avoid problems that could be introduced by heterogeneity of M_c , we usually map M_c to

define the spatial extent of the high-quality part of the catalog and restrict our analysis to that area [e.g., *Wiemer and Wyss*, 2000].

By mapping M_c for various periods, we can determine what area is covered at an approximately uniformly low M_c . In the selection of M_c , we must choose a compromise that allows the coverage of the area of interest (or maximizes the area), but also does not unnecessarily reduce the number of events available. Thus, the boundary of the study area is determined based on objective criteria, and is not a free parameter. An example of a map of M_c for the western US is shown in Plate 2C. M_c ranges from > 2.5 offshore at Mendocino to < 1 in central California.

We generally do not use hypocenter accuracy as a measure of catalog quality, because the individual sample volumes we use (1 km beneath volcanoes, 5 to 30 km along fault zones) are larger than the errors, and thus it usually is not a critical issue in our work. In those cases where the hypocenter errors may vary in space and may be comparable to the dimensions of the sampling volumes, the problem of hypocenter error has to be studied carefully to decide whether or not b -value mapping is meaningful.

2.5 Homogeneity of reporting with time

In most catalogs, earthquakes are not reported homogeneously with time [*Habermann*, 1982; *Habermann*, 1987; *Zuniga and Wiemer*, 1999; *Zuniga and Wyss*, 1995] because the data gathering and analysis methods change. Cases where the cause of these changes has been identified are described by *Wyss* [1991] and *Pechmann et al.* [2000], for example.

It is not easy to discover possible shifts or stretches in the magnitude scale, because these may vary as a function of space, as, for example, in offshore and onshore areas. We attempt to handle the problem by searching for significant reporting changes, using the algorithm GENAS [*Habermann*, 1983] in areas we judge likely to share major catalog characteristics. It is rare that duplicate catalogs are available to verify the interpretation of changes we detect by GENAS [*Habermann and Craig*, 1988]. Simply comparing the FMD for two periods in either the cumulative or non-cumulative form can yield important clues about artifacts. An example of a magnitude shift taken from the Tohoku region of Japan is shown in Figure 4 [*Wyss and Toya*, 2000]. Crosses and circles mark the two periods compared (1988.7-1991.1 and 1984.3 – 1987.3, respectively). The data in the later period are systematically shifted toward smaller magnitudes, suggesting that around 1988 a change in the magnitude scale occurred.

Often, catalogs are reasonably homogeneous, starting when the network was improved to its modern state. This allows us to use the data without modification from t_s on. In cases where simple magnitude shifts are detected, without changes in average b -value, one may be able to introduce corrections of the magnitude scale during selected periods, and thus avoid shortening the data set. The successful modeling of magnitude shifts by *Wyss and Toya* [2000] has shown that our interpretation of shifts and their correction is a viable means of repairing heterogeneous reporting.

Magnitude stretches are more difficult to identify as artificially introduced, because they could be due to natural changes of b -values. The criteria we use to interpret a change in b -value as an artificial magnitude stretch is that (a) it occurs in a large area, and (b) at a time without a major tectonic event, and (c) possibly at the time of known innovations introduced in the seismograph network operation. For b -value mapping, data sets containing apparent magnitude stretches cannot be used; the data period must be shortened to exclude the suspected stretch.

2.6 Contamination by explosions

Explosions, mostly quarry blasts, frequently contaminate seismicity data. If they are present, they bias the b -estimates locally toward large values, because, on average, explosions are smaller than earthquakes and of similar sizes. Since explosions usually take place during daytime hours, a histogram of the earthquakes in a region broken down by the hour of the day can show a telltale peak during daytime hours (Figure 5). Consequently, areas where explosions occur frequently can be identified by the ratio, R_q , of day- to nighttime earthquakes [Wiemer and Wyss, 2000]. An example of an R_q map for Alaska is shown in Figure 5. Because we usually do not have the resources to identify individual explosions by signal analysis, the only choice for cleansing the data is to eliminate the areas in which explosions are frequent. This leaves holes in the region selected initially for study, in which there is no information on b - or a -values. However, this is preferable to contamination of the results through the presence of explosions. In some cases, the contamination by explosions may be so pervasive that the most sensible solution is to limit the analysis to nighttime events only.

2.7 Magnitude scales

Different magnitude scales, such as M_L , M_D , m_b , M_s , and M_w , are in use. If an area is monitored by two or more networks, one often finds that the absolute b -values between networks vary. If a network provides a mixture of magnitudes, one can aim to translate one into the other by finding a regression based on the events reported with both magnitudes; however, the scatter in these transformations is commonly large and systematic errors may be intro-

duced. To map the b -value, we consider it best to analyze network data independently, and, if possible, confirm spatial or temporal patterns discovered in b through independent data sources.

Because the magnitude scale is defined arbitrarily, it has no physical meaning and the b -slope cannot be directly related to source dimensions. Therefore, it would be desirable to investigate the slope, β , of the frequency-moment, M_o , distribution because in this case the abscissa has a physical meaning [Kagan, 1999; Wyss, 1973] and can be related to the dimensions of the ruptures. However, information on M_o is currently limited to large earthquakes worldwide (Harvard moment tensor catalog) and to very local catalogs [Nadeau and McEvilly, 1999]. A strategy to derive some rough information might be to convert M into M_o by an average equation and study the resulting β . However, the scatter in data sets for which M and M_o are known is very large, which implies that earthquakes have vastly different stress drops. In this case the distribution of numbers of events as a function of M_o cannot necessarily be retrieved faithfully from data for which only M was measured. For these reasons, we have not yet mapped and analyzed β .

3. Method

3.1 Mapping the seismicity

To visualize the frequency-magnitude distribution as a function of space, the earthquakes are projected onto a plane. We estimate the b -value at every node of densely spaced grids, using the N nearest earthquakes, or a constant radius, R . N is constant and usually in the range of 50 to 500 and the nodal separation is typically 0.5 - 10 km. The sampling volumes have the shape of cylinders with a vertical axis. Volumes overlap and their sizes are inversely proportional to the local density of epicenters. The grid we interactively create excludes areas of low seismicity to save computing time. The b -value is estimated for each volume, the corresponding value translated into a color code and plotted at each node.

Alternatively, we use the equivalent approach to analyze cross-sections. A cross-section of given depth is interactively defined and all hypocenters projected onto a plane. The sampling volumes are consequently cylinders with a horizontal axis. Figure 6 demonstrates the mapping approach for a 10 km wide cross-section along the Parkfield segment of the San Andreas fault. The top frame shows the hypocenters. The middle frame shows the nodes with a 1 km spacing, and some of the sampling volumes are plotted as circles. The bottom frame contours the radii of the sampling cylinders, ranging from 0.5 to 10 km. Light gray indicates a high spatial resolution, dark colors a low resolution.

For both, map view and cross-section, the sampling volumes can assume shapes that are undesirable. In areas of low seismicity, coin-shaped sample volumes may be neighboring pipe shaped ones in areas of high seismicity. This may or may not be desirable. Alternatively, a true three-dimensional gridding can be used. At each node of a three dimensional grid, we sample the nearest neighbors in three-dimensions, resulting in spherical sampling volumes of either constant sample size or constant radius. This approach is best suited for areas of distributed seismicity.

3.2 Computing the b -value and its uncertainty

Numerous studies have been devoted to estimating b and its uncertainty [Aki, 1965; Bender, 1983; Frohlich and Davis, 1993; Guttorp, 1987; Guttorp and Hopkins, 1986; Kijko and Sellevoll, 1989; Okuda et al., 1992; Page, 1968; Rhoades, 1996; Shi and Bolt, 1982; Tinti, 1989; Tinti and Mulargia, 1987]. The b -value is in our cases studies calculated by the most commonly used maximum likelihood method [Aki, 1965; Hamilton, 1967], which has been shown to be a robust and unbiased estimation of M_c in most cases [Bender, 1983; Wiemer and Wyss, 1997]:

$$b = \log_{10}(\text{exp}) / (M_{\text{mean}} - M_{\text{min}}) \quad (3)$$

where M_{min} is the minimum magnitude to which the FMD is defined and M_{mean} the mean magnitude. Note that M_{min} needs to take the effect of the discrete binning of magnitudes into account. If the binning is 0.1 magnitude units, $M_{\text{min}} = \min(M) - 0.05$ [Utsu, 1978]. An estimate of the standard deviation δb of the b -value can be obtained using the equation first derived by Aki [1965], or the improved formulation by Shi and Bolt [1982]

$$\delta b = 2.3b^2 \sqrt{\frac{\sum (M_i - \langle M \rangle)^2}{n(n-1)}} \quad (4)$$

where n is the sample size. We commonly estimate the probability that two samples may come from the same population by Utsu's [1992] test.

$$P \approx \exp(-dA/2-2) \quad (5)$$

where $dA = -2N \ln(N) + 2N_1 \ln(N_1 + N_2 b_1/b_2) + 2N_2 \ln(N_1 b_2/b_1 + N_2) - 2$ and $N = N_1 + N_2$. This test accounts explicitly for the number of earthquakes contained in each sample. By using small samples to map b , one gains resolution but is penalized with lower probabilities that mapped anomalies are significant. To establish the significance of differences between two b values requires that they be different at the 95% confidence limit or higher.

Temporal changes of b values can be mapped by "differential b value maps" in the following fashion [Wiemer *et al.*, 1998]: (1) Calculate a b -value grid for the period T_1 - T_2 , as described above, but using constant size volumes. (2) Calculate a b -value grid for the period T_3 - T_4 , using the nodes and volume size defined in (1). (3) Compare the frequency-magnitude distributions at each node for the two periods. (4) Map the difference in b -value at nodes where it is statistically significant at the 95% confidence level as measured by *Utsu's* [1992] test (equation 5). These differential b -value maps thus identify volumes of significantly increased or decreased b -value.

4. Case studies of mapping the b -value in various tectonic regimes

4.1 Volcanoes and geothermal fields

It has been generally known for a long time that b -values beneath volcanoes are elevated, but it was a surprise when *Wiemer and McNutt* [1997] showed that beneath Mount St. Helens and Mt. Spurr the high b -values were concentrated in small volumes ($r \approx 1.5$ km) and the rest of the crust showed normal to low values. Since then, we have mapped similar small, anomalous volumes beneath Off-Ito volcano [Wyss *et al.*, 1997], Long Valley and Mammoth Mountain [Wiemer *et al.*, 1998], Montserrat [Power *et al.*, 1998], Etna [Murru *et al.*, 1999], Katmai [Jolly and McNutt, 1999], Mt. Redoubt [Wiemer *et al.*, in preparation] and adjacent to the east rift zone of Kilauea [Wyss *et al.*, 2001a] (Plate1). In all cases, high b -value volumes ($b > 1.3$) can be identified clearly, embedded in a background of normal b ($b \leq 1$).

The most basic conclusion is that the b -value underneath volcanoes is not as previously thought generally higher, but that pockets of anomalously high b -value are embedded in average crust. These anomalies are highly significant and in general cannot be explained through problems in the catalog.

Comparing the anomalies of high b -values with other geophysical and geodetic data regarding the location and extent of magma chambers, we came to the following conclusion: In the seismogenic vicinity of magma chambers located by independent studies, we always find high b -values. Additional anomalies of high b -values exist, particularly at shallow depths. In these cases, we do not know for certain if magma is associated with the b -value anomalies. However, the absence of an anomaly fairly strongly suggests the absence of magma. Other factors causing high b -values may be the presence of hot fluids in geothermal systems, or extensive cracking, which a volume may have acquired during past eruptions.

Of course, magma chambers and volumes containing partial melt are not capable of generating earthquakes. The anomalies we map must reside in the volumes surrounding what

we call “magma chambers,” although we cannot distinguish between a volume such as a plexus that might be crisscrossed by dikes, a volume that contains partial melt, or a mostly liquid volume. Because the anomalous volumes generally have dimensions approximately equal to the errors in the hypocenter locations, and because of the limited number of earthquake available for mapping, we cannot map the anomalies as rings around a central body not containing any events. This may become possible in the future with new high-resolution hypocenter location techniques.

In the vicinity of a magma chamber embedded in the crust, one expects high heterogeneity, high pore pressure and a high thermal gradient. All these parameters have been linked in the laboratory to high b -values.

In many of the volcanoes studied so far, the b -value anomalies are not located straight below the summit (Off-Izu, Etna, Mammoth, Kilauea east rift zone, Redoubt), which suggests that complex magma conduits are perhaps more common than simple ones. The depths of the “chambers” mapped ranged from 1 to 13 km, and several volcanoes showed anomalies at more than one depth (Mount St. Helens, Etna, Mammoth), also indicating that magma supply systems are often complex.

4.2 Mapping Asperities

The concept that faults consist of locked segments that resist faulting (asperities), unlocked segments characterized by creep, and segments with intermediate properties, is generally accepted. In the creeping segments, stresses are largely relieved so they cannot build up, whereas in asperities stresses are concentrated. Most main shock energy emanates from the asperities, while the creeping segments may participate in a main rupture by smaller amounts of co-seismic slip. A rupture may involve only one asperity and stop as major earthquake, or it may reach one or several neighboring asperities, and continue to generate a large to great earthquake. Whereas it is clear that the above model applies to many fault ruptures, the reasons for the difference in resistance to failure are not firmly established. Varying pore pressure is one parameter that is capable of causing the observed differences in locked and unlocked segments [Byerlee and Savage, 1992; Miller, 1996; Nur, 1973; Rice, 1992].

Given the fault model described above, one should expect variations in a - and b -values in different fault segments because fault properties and stresses vary. Testing this idea along the San Andreas fault near Parkfield yielded a strong contrast between b -values in the creeping segment and the asperity beneath Middle Mountain [Amelung and King, 1997; Wiemer and Wyss, 1997] (Plate 2A). We found that this pattern was surprisingly stable during the period of available data (1973-2000.5) (Plate 2B), and that the magnitude distribution and

productivity level can be predicted from past activity [Wiemer and Wyss, 2001]. This is illustrated in Figure 7, where we compare the frequency-magnitude distribution observed in the creeping segment of the San Andreas fault with the one in the asperity. The two distributions are distinctly different in each of the periods analyzed. Based on the data from 1981 to 1996 (Figure 7B), we forecast the distribution of earthquakes represented as solid lines in Figure 7C in the two contrasting volumes. These forecast distributions are confirmed by the events that occurred in the last 4.2 years (triangles and squares in Fig. 7C). In particular, the two largest events that occurred in the last 4.2 years were located in the volumes where they were forecast by the data through 1996.

Having discovered that b -values are strongly heterogeneous, and being aware of the well-known variations of the a -value in equation 1, we realized that the local recurrence time, T_L , must also vary strongly. T_L is estimated for seismic hazard assessments by extrapolating the frequency magnitude relationship observed over a period, ΔT , to a target magnitude of M_{targ} by

$$T_L = \Delta T / (10^{(a-bM_{targ})}) \quad (6)$$

The inverse of T_L , calibrated by the area from which the data are extracted, is the annual probability per km² for an earthquake with the target magnitude

$$P_L = 1/T_L/A \quad (7)$$

Thus, the second step in our analysis is to map the a -value and combine the information contained in it with that of the local b -value to estimate P_L (alternatively T_L). By doing this, the image of the asperity beneath Middle Mountain becomes very sharp (Plate 2A) and conforms precisely to the definition of this asperity by other means [Bakun and McEvelly, 1984].

The earthquake catalog for the San Jacinto-Elsinore fault system provided an excellent testing case for the hypothesis that asperities may be mapped by T_L (P_L) because the catalog since 1981 contained no earthquakes larger than $M_{4.9}$, but the locations and approximate extents of six historic shocks in the range $5.8 < M_L < 6.8$ are known. We estimate that the result that five of the six main shocks correlated with anomalies in P_L (Plate 3D), although the area covered by these anomalies was only about 10%, has a probability of about 10^{-3} to occur by chance [Wyss *et al.*, 2000].

A similar result was found for the Tokai-Kanto area, where again 5 out of 6 main shocks ($M \geq 6.5$) correlated with areas of anomalously large P_L , covering about 14% of the total area studied [Wyss and Matsumura, 2001]. The 1923 Kanto earthquake that destroyed

Tokyo emanated from the largest anomaly found. At least one, possibly two, anomalies exist at the estimated ends of the expected Tokai earthquake.

Along the Pacific margin of Mexico, the plate boundary segment offshore of Chiapas shows anomalously high P_L . As this part of the plate boundary was seldom considered in publications concerning seismic hazard, we investigated its history and found that five $M \geq 7$ shocks had ruptured this segment since 1903, with an average return period of 23 years [Zuniga and Wyss, 2001]. The fact that the analysis drew our attention to a plate boundary segment with a short historic recurrence time, but that was not known as unusually active, suggests that the method is useful.

In the case of the 1999 Izmit $M7.4$ earthquake [Westerhaus *et al.*, 2001] had identified a volume only 10 km from the epicenter as the most likely location for a main shock a year before it occurred, on the basis of a b -value anomaly in an earthquake catalog covering the eastern part of the rupture. This pre-main shock assessment of the earthquake potential along this part of the North Anatolian fault was contained in a report to the funding agency and in a manuscript submitted for publication in 1998. After the Izmit main shock, Oencel and Wyss [2000] found that the earthquake catalog covering the western part of the rupture contained a b -value anomaly at the western end of the 1999 rupture, suggesting that this rupture may have been arrested by a locked fault segment, not yet under sufficient stress to continue rupturing.

The reason for the low b -value is likely the state of stress near an asperity (a strong and homogeneous stress field). Creeping segments of faults on the other hand display high b -values. The local recurrence time for moderate main shocks of neighboring sub-volumes varies by several orders of magnitude depending on the local b - and a -value. The fact that the local recurrence times measured in the asperity volumes agree reasonably with the historical and paleoseismic record [Wyss *et al.*, 2000; Zuniga and Wyss, 2001] suggests that recurrence of main shocks is timed by processes in the asperity volume. Neighboring creeping segments do not contain information about the recurrence time of main shocks. Combining information from these two distinctly different regions into one recurrence time calculation, results in overestimates.

4.3. Mapping temporal changes of earthquake probability

Assuming that the frequency-magnitude relationship may be extrapolated to large earthquakes, we can calculate the local recurrence time $T_L(M_{max})$ by equation 6, and the local probability by equation 7. If the redistribution of stress due to a large earthquake leads to a

change in one or both of the parameters a and b , then the T_L and P_L will also change. Because the seismicity rate increased strongly after the Landers $M7.3$ earthquake of 1992 in several parts of California during the following several months, arguments were put forth to show that static, as well as dynamic stress changes played a role in triggering the additional seismicity [Gomberg and Davis, 1996; Gomberg et al., 2000; Hill et al., 1995; Stein et al., 1992].

A short lived change in seismicity rate that lasts only months would not lead to a change in P_L , according to our hypothesis, because we classify this short-term increase in activity as a cluster, like an aftershock sequence. However, the Landers earthquake changed the background seismicity rate in a positive as well as negative sense in neighboring volumes for at least seven years following it (Plate 2E(A)), which made a recalculation of P_L after Landers necessary [Wyss and Wiemer, 2000b]. In addition, it appears that the Landers earthquake also changed the b -value in many parts of southern California (Plate 2E(B)). Thus, we calculated the T_L and P_L based on the declustered catalog for the 12 years before and for the seven years following Landers and mapped the difference [Wyss and Wiemer, 2000]. Plate 2E(C) shows that P_L decreased strongly in some volumes, but increased in others. One of the strongest increases in P_L is observed in the northern part of the source volume of the $M7.1$ Hector Mine earthquake of 1999.

4.4 Changes of b with depth in California

Three recent studies have addressed the change of the b -value with depth in the seismogenic crust in California. Wiemer and Wyss [1997] noted that the b -value in the Parkfield and Morgan Hill regions systematically decreases from high $b > 1.1$ in the top 5 km to $b < 0.8$ below 6 km depth (Figure 8). Mori and Abercrombie [1997] confirmed this decrease with depth for several other regions in California, and proposed that the lower b at depth corresponds to a higher probability of larger earthquake to nucleate at depth. In a systematic test, Gerstenberger et al. [2001a] separately mapped the areas in southern and northern California where a statistically significant decrease can be observed. In about one-third of the area investigated, this decrease of b with depth can be established at the 99% confidence level. The opposite pattern, an increase of b with depth, was only found for about 1% of the nodes, the remainder had no change with depth or insufficient data to establish significance (Plate 2D).

Based on these studies, we believe that for California, a decrease of b with depth has been firmly established. The physical cause of this decrease, however, has not been established with certainty. We speculate that the change of ambient stress with depth plays an im-

portant role. The top 5 km in this model are weakly coupled and cannot buildup significant amounts of shear stress, resulting in a high b -value.

4.5. Mapping b in subducting slabs

Although it is not a surprise that b varies in the heterogeneous crust, one might assume that deep seismic zones may be more homogeneous and do not show significant variations. However, *Wiemer and Benoit* [1996] mapped well-defined anomalies ($b > 1.2$), similar to those found in the crust at a few kilometers beneath volcanoes, at about 100 km depths, in the subduction zones of Alaska and New Zealand. They interpreted these anomalies as due to dehydration of the descending oceanic crust at the top of the slab and proposed that their locations mark the origin of magma, feeding subduction zone volcanism.

In northeastern Japan, the anomaly is located at 150 km depth, tens of kilometers to the west of the volcanic arc. Detailed seismic tomography revealed a low velocity zone that connects the b -value anomaly in the descending slab at 150 km depth with the b -value anomalies directly beneath the volcanoes at 30 km depth by an inclined path [*Wyss et al.*, 2001b] (Plate 3B).

Detailed mapping of the b -value in segments of the deep seismic zones with the best data (Japan and Alaska) showed that the extent and strength of the b -anomalies in the depth range of 80 to 150 km varies along the strike of the subduction zone, and that another anomaly exists at 400 km depth in Japan [*Wyss et al.*, 2001b].

4.6. Variations of b in aftershock sequences

In addition to investigating the b -value, the decay rate of aftershocks is also of interest. It is often described through the parameter p in the modified Omori law:

$$R(t) = \frac{k}{(t+c)^p} \quad (8)$$

where $R(t)$ is the rate of occurrence of aftershocks, and k , c , and p are constants [*Kisslinger and Jones*, 1991; *Omori*, 1894; *Utsu et al.*, 1995].

When investigating b -values of aftershock zones, it is particularly important to carefully study first the temporal changes of M_c . Within the first hours to days of an aftershock sequence, M_c tends to decrease systematically. This is caused by improvements of the station network and the fact that the frequent larger aftershocks mask small events.

In Plate 3A, we show a map of the b -value after the $M7.3$ 1992 Landers and $M7.1$ 1999 Hector Mine main shocks [*Wiemer et al.*, 2001]. Low b -values are found south of the

Landers hypocenter, and north of the Hector Mine hypocenter. In both cases, the lowest b -value areas are located outside the rupture area of the main shock. It is tempting to propose that the slip distribution during the main shock and its resulting stress distribution may control the size distribution within the aftershock sequence; however, we have yet to establish this correlation quantitatively [*Wiemer and Katsumata, 1999; Wiemer et al., 2001*].

The analysis of the spatial distribution of the b and p values within five aftershock zones (Landers, Hector Mine, Northridge, Kobe, and Morgan Hill) suggests that these parameters vary strongly [*Wiemer and Katsumata, 1999; Wiemer et al., 2001*]. Therefore, the common practice of simply assigning an overall p and b value to an entire aftershock sequence is an oversimplification of the complex and spatially heterogeneous internal structure of aftershock sequences. This should not come as a surprise, since the physical parameters governing the decay rate and size distribution, such as stress, material properties, pore pressure etc., are likely to vary substantially along the strike of an extended aftershock zone. The aftershock seismicity in one section of the fault can be considered as largely independent from the activity at another end. Just as a large main shock cannot be treated as a point source when studying effects within the near field, our results show that we need to investigate spatial variations of these seismicity parameters within the aftershock zone. We propose that spatial variations in b - and p -values are characteristic for all aftershock sequences of moderate to large earthquakes.

4.7 Implications for aftershock hazard

Aftershocks may pose a significant hazard in populated areas, and at the same time offer a rich source of information for seismicity studies. Measures have been implemented to assess this hazard in near real time to assist government, industry, and emergency response teams in decisions such as determining when it is safe to demolish, repair or allow people to use damaged structures [*Hough and Jones, 1997; Reasenber and Jones, 1989; Reasenber and Jones, 1990; Reasenber and Jones, 1994*]. Probabilistic aftershock hazard assessment is based on the two power laws that describe the temporal behavior of an aftershock sequence: The modified Omori law and the Gutenberg-Richter relationship. From these power laws, one can obtain an equation [*Reasenber and Jones, 1989; Reasenber and Jones, 1990; Reasenber and Jones, 1994*] that describes the rate $\lambda(t, M)$ of aftershocks of magnitude M or larger:

$$\lambda(t, M) = 10^{a+b(M_m-M)}(t+c)^{-p} \quad (9)$$

where t is the time after the mainshock and M_m the mainshock magnitude. By modeling the aftershock sequences as Poisson process with a time-dependent rate parameter (Reasenber, 1985), one can derive the probability P of one or more earthquakes occurring in the magnitude range ($M_1 \leq M < M_2$) and time range ($S \leq t < T$):

$$P = 1 - \exp\left(-\int_T^S \lambda(t, M) dt\right)_{M_1}^{M_2} \quad (10)$$

Since all three parameters, the a -, b - and p -value, vary significantly within individual aftershock sequences, the aftershock hazard also varies. This hazard can either be expressed as a spatially and temporally varying forecast of an aftershock above a given magnitude threshold, or by computing time-varying probabilistic aftershock hazard (PAH) maps [Wiemer, 2000]. These PAH maps have been investigated in a retrospective study for the Landers sequences [Wiemer, 2000] and in a near-real time mode for the Hector Mine earthquake [Wiemer et al., 2001]. In both case studies, PAH maps have been shown capable of reasonably portraying the aftershock hazard, with the highest hazard to the south of the Landers rupture, and the north of the Hector rupture. A systematic test of the capabilities and limitations of PAH maps is currently under way [Gerstenberger et al., 2001b]. The pattern of highest hazard for the Landers and Hector Mine sequences is interestingly directly reversed to the observed triggering of small aftershocks at larger distances [Gomberg et al., 2001; Harris and Simpson, 1992], suggesting that static, and not dynamic transfer of stress through the mainshock is governing aftershock hazard; However, the current static stress triggering models [Hardebeck et al., 1998; King et al., 1994; Stein et al., 1992] cannot explain the distribution of aftershock hazard nor the distribution of seismicity.

4.8 Spatial variations of b on regional to global scales

While the evidence for spatial variability in b is overwhelming on a local to regional scale, there continues to be doubt about the regional to global scale. Studies by Frohlich and Davis [1993] and Kagan [1999] suggest that there is little variation of b between different tectonic regions and that the observed differences are at least partially due to artifacts, rather than natural. The spatial resolution of these studies is on the order of several hundreds to thousands of km. In a recent study of the Himalayan region, on the other hand, Regenauer-Lieb and Wiemer [2001, personal communication] do find spatial variability of b on this scale (Plate 3C). High b -value regions are found near the singularities of the indenter (India) that penetrates into the Eurasian plate. We speculate that the fact that spatial variations of b on

large scales have not often been established could be due to (1) the lack of high quality earthquake catalogs with low M_c on this scale; (2) the lack of rigorous studies; or (3) because heterogeneity in the Earth exists primarily on smaller scales.

5. Changes of b -values as a function of time

Many authors have investigated temporal changes of b . Most of these studies addressed bulk changes rather than temporal changes in sub volumes; however, some studies have investigated both spatial and temporal variability of b simultaneously [Ogata *et al.*, 1991]. In mines, temporal variations in b have been used for time varying hazard analysis [Gibowicz and Lasocki, 2001], whereas the application to larger scale tectonic systems remains speculative [Knopoff *et al.*, 1982; Knopoff *et al.*, 1996; Smith, 1998]. In our research, we found that lasting and significant changes of b -value as a function of time are not common. In our efforts to spatially map b , we searched for temporal changes, but could generally not find substantial and lasting changes. In one of the best data sets at Parkfield, b is remarkably stable with time (Figure 2B). However, major events such as magmatic intrusions and large earthquakes do change b locally. Beneath the Off-Izu volcano, we noticed a three phase increase in b , correlating with three intrusions [Wyss *et al.*, 1997]. To document the change associated with the 1989 intrusion beneath Mammoth Mountain, we improved the technique by mapping the change [Wiemer *et al.*, 1998]. In this case, the change had a maximal amplitude of $\Delta b=0.6$ near the shallow termination of the intrusive dike, but extended to about 2 km depth at a reduced amplitude of $\Delta b=0.2$ (Figure 9).

The three cases in which we documented a temporal b -value change with high statistical significance were all step-function-like increases and associated with a major redistribution of stress, or injection of fluids into the seismogenic volumes. However, long-period changes may also occur. Jones and Hauksson [1997] showed that the b -value in Southern California was lower before the 1952 Kern County earthquake than after it. The hypothesis that the seismic moment release increases regionally before large earthquakes [Varnes, 1989] implies that b should be anomalously low before them [e.g., Bowman *et al.*, 1998].

The differential b -value map after the 1984 Morgan Hill main shock (Figure 10) shows that a change in b only occurred near the area of largest slip [Wiemer and Katsumata, 1999]. Therefore, we propose that although it is easy to change the productivity of a volume (the a -value), it is much more difficult to change its b -value. This explanation is consistent with the physical interpretation of b as an expression of homogeneity in stress and material properties, since it is not easy to change these properties.

Precursory changes of b -values before mainshocks

Early investigations of the possibility that the FMD may change before main shocks were hampered by inferior data quality, but the suggestion that during a pre-shock-fore-shock period the mean magnitude increased (b decreased) was supported by some data [Main *et al.*, 1989; Narkunskaya and Shnirman, 1994; Smith, 1986; Smith, 1990; Wyss and Lee, 1973]. Recently interest in this topic has been revived [Rotwain *et al.*, 1997; Smith, 1998]. Several observations show that b -values before main shocks are different than after them, or than during the background period [Jones and Hauksson, 1997] [Bowman *et al.*, 1998; Wyss and Wiemer, 2000, Knopoff *et al.*, 1982; Knopoff *et al.*, 1996].

6. Fractal dimension and b -value

It has long been speculated that the distribution of earthquake in space and their size distribution are related. The fractal dimension, D , of hypocenters is one convenient measure of the distribution of hypocenters in space. D was found to follow a power law [Kagan, 1991; Kagan and Knopoff, 1980; Robertson *et al.*, 1995; Turcotte, 1992; Volant and Grasso, 1994], hence exhibit a self-similar scaling. Assuming that the seismic moment, M_0 , is proportional to fault dimension cubed, and that the spatial distribution of earthquakes is fractal, [Aki, 1981] showed that then the fractal dimension D and b -value should be related as

$$D = \frac{3b}{c} \quad (11)$$

where $c \approx 1.5$ is the scaling constant between log moment and magnitude [Kanamori and Anderson, 1975]. If a more general relationship between moment and fault length L ($M_0 \propto L^d$) is assumed [King, 1983] generalized equation (1) to

$$D = \frac{d}{c} b \quad (12)$$

For small earthquakes with circular rupture areas, $d=3$, as in (10) and $D=2b$. For large earthquakes that span the crust and only extend laterally, $d=2$ and $D = \frac{4}{3} b$.

For the Parkfield data set there is specific information on these constants. Nadeau and Johnson [1998] observed that the period T of repeating earthquakes scales as $T \propto M_0^{1/6}$. For non-interacting asperities, continuity of fault displacement requires the same average displacement rate on all asperities, i.e. $\bar{d}/T = \text{constant}$, independent of moment. Hence $\bar{d} \propto M_0^{1/6}$. Since $M_0 = GA\bar{d}$, this leads to $A \propto M_0^{5/6}$ or, equivalently, $M_0 \propto (L^2)^{6/5} = L^{2.4}$ which, by defini-

tion, gives $d=2.4$. In addition, an independent determination of magnitude and moment for the events [Samis et al, 2001] yields $\log_{10} M_0 = 1.6M + 15.8$. Thus $c = 1.6$ for Parkfield events. Hence, based on the Parkfield data itself, we expect $d/cF = 2.4/1.6 = 1.5$.

A critical issues when determining D is hypocenter accuracy, $\Delta L(x,y,z)$, since D should not be determined based on values less than ΔL [De Luca et al., 1999; Harte and Vere-Jones, 1999; Nerenberg and Essex, 1990]. Similar to the estimation of completeness in magnitudes, estimating ΔL is not simple and incorrect estimation of ΔL can lead to significant errors in D .

Hirata [1989] disagreed with equation (11) based on measuring both the b -value and fractal dimension of the hypocenters of shallow (0-60 km) earthquakes located off shore east of Japan as a function of time. However, the catalog used by Hirata is not homogeneous in the reporting of magnitudes, or in epicenter accuracy, over the period he used (1923 to 1986), and each measurement of D and b was based on 100 events only. Many of the epicenters are uncertain to at least 20 km, which suggests that the results may not be reliable. Sammis et al. [2001] concluded, on the basis of an earthquake catalog with hypocentral errors of 0.2 km, that along parts of the San Andreas fault equation (11) holds.

The question of how well the distribution of earthquakes in space approaches a fractal distribution, and how well equations (11) and (12) describe the relationship of D with b , is of fundamental interest, but currently still open. We expect that it will be answered in detail, as more high quality data sets become available.

7. The physical processes perturbing b -values

The data from underground mines [Urbancic et al., 1992; Gibowicz and Lasocki, 2001] and a gas field [Lahaie and Grasso, 1999] are the most convincing, linking decreases in b -value to increased ambient stress and increased stressing rate, respectively. The correlation of high pore pressure with high b -values also links low b -values to higher stress, but so far the data are weak [Wyss, 1973]. In addition, laboratory experiments support the same conclusion [Scholz, 1968]. Also, the conceptual model is convincing that earthquakes are more likely to grow into larger events in a highly stressed medium, because the difference between volumes of maximum and minimum stress is small and can be overcome more easily by a propagating rupture than in a low-stress volume with deep energy wells that a rupture must overcome to continue. Furthermore, the rapid (one to a few months) and massive ($\Delta b \sim 0.4$) increase in b -values at several kilometers distance from a magmatic intrusion is well explained, assuming

an increase in pore pressure [Wiemer *et al.*, 1998]. We also find a correlation of the average stress tensor misfit and the b -values [Wiemer *et al.*, 2001]. Finally, the observed decrease in b -value as a function of depth in California [Gerstenberger *et al.*, 2001; Mori and Abercrombie, 1997; Wyss, 1973] can also be interpreted as due to increasing ambient stress level. Taken together, these lines of evidence support the interpretation that b -values can be perturbed by differences in ambient stress. Nevertheless, the correlation of low b -values with high stresses needs to be strengthened by additional high quality observations.

The alternative explanation that high b -values may be due to increased structural heterogeneity [Mogi, 1962] cannot be ruled out and is supported by some data [Westerhaus *et al.*, 2001]. Although this line of evidence is not strongly developed, it is likely that both factors, structural heterogeneity and stress level, can perturb the b -value.

The idea that b -values may be influenced by temperature is supported by only one sequence of laboratory experiments [Warren and Latham, 1970], and it seems difficult to test it in the field. In our discussions, we tend to give it less weight than the two aforementioned possibilities because of the paucity of information about it, but we cannot rule it out as another feasible mechanism.

8. Common problems and complications

8.1. *Catalog heterogeneity* as a function of time can be a serious problem for identifying b - and a -value changes with time. Although careful analyses, using the techniques we have developed, can detect some artificial reporting changes [Pechmann *et al.*, 2000; Wyss, 1991; Wyss and Toya, 2000; Zuniga and Wiemer, 1999; Zuniga and Wyss, 1995], others may go undiscovered.

8.2. *The lack of a unique physical interpretation* of anomalies may remain a problem, even if more correlations to specific causes can be established, because it may well be that more than one parameter can influence the b -value.

8.3. *Selective hypocenter location errors* as a function of magnitude might sort small and larger microearthquakes into different volumes. Because the b -value anomalies beneath volcanoes often have radii of about 1 km, the systematic error thus introduced may be large enough to mimic an anomaly where there is none.

8.4. *Magnitude scales can differ.* This can lead to problems within a region and between regions.

(a) Microearthquakes from which the b -value is derived are commonly measured by duration magnitudes, M_D . In spite of the best efforts of network operators, this scale is often

not the same as the M_S scale, on which main shocks are measured. In this case, local **differences** in earthquake potential (T_L and P_L) can still be defined, but the absolute values for T_L and P_L are incorrect because they depend on the extrapolation from the M_D data set [Zuniga and Wyss, 2001].

(b) In some regional networks, it may not be known that the attenuation properties are anomalous. This can lead to a regional M_D -scale that is substantially stretched (or compressed) with respect to the original M_L -scale, as defined in California [Gutenberg and Richter, 1954]. In that case, the b -value range may be unusual ($1 < b < 3$, for example [Oencel and Wyss, 2000; Westerhaus *et al.*, 2001]. We do not interpret the observation of a regionally shifted b -range to mean that the entire region is anomalous, but assume that the magnitude scale differs from the standard. In this case also, the **differences** in local b -values can still be defined reliably, and inferences on locations of asperities or magma chambers may be drawn.

8.5. The methods can only be applied to seismically active volumes.

Beneath volcanoes, where earthquakes are often restricted to very small events ($M < 2$), b -values can only be mapped if local networks provide detailed catalogs. Also, large magma bodies and locked fault segments may produce no earthquakes and cannot be mapped.

In many catalogs, the number of earthquakes per unit volume available is marginal, and may allow a resolution for mapping that is coarser than the heterogeneity actually present. For example, beneath Etna most of the radii containing sufficient events for estimating b exceeded 2 km [Murru *et al.*, 1999], whereas we would have liked to map this volume with $r < 1$ km, to resolve the images of the two anomalies sharply. Similarly, we were forced to use $r = 20$ km to map anomalies in the Kanto-Tokai area [Wyss and Matsumura, 2001], although asperities for $M \geq 6.5$ main shocks may be substantially smaller and not crisply resolved by our analysis, until more time has elapsed so that the catalog contains more events.

8.6 Bi-modal distributions of magnitudes

In some volumes of the Earth, the assumption that the FMD can be adequately described as a power law is clearly invalid [Knopoff, 2000; Pacheco *et al.*, 1992; Trifu *et al.*, 1995]. This breakdown of a power law scaling is, for example, often observed in volcanic regions, where earthquake swarms and families introduce a non-power law population of events of very similar size. A sample FMD in non-cumulative form is shown in Figure 11. The excess of $M \sim 1.3$ earthquakes is caused by a self-similar family of events which are likely not earthquakes but vibrations of a crack or pipe. In other cases, contamination by explosions can introduce an apparent bi-modal scaling. [Wiemer and Wyss, 2000] documented for a case

study in Hokkaido [Taylor *et al.*, 1990] how temporal and spatial variability in M_c can be misinterpreted as an apparent breakdown in scaling.

When mapping b -values, it is vital to look out for areas where a power law scaling is not appropriate. These areas might be found by their poor fit of the FMD to a power law. In addition, bi-modal areas can sometimes be identified as anomalies in M_c maps. Using automatic mapping, bi-modal FMDs can be misinterpreted as either an unusually low or high b -value, depending on the estimate of M_c . Therefore, inspecting both maps of M_c and of the goodness of fit to M_c is indispensable before trusting a b -value map, and selected interactive screening of the individual FMD's for bi-modal distributions is advisable.

9. New hypotheses and preliminary conclusions

9.1. Hypothesis I: Active magma chambers in seismogenic crust may be mapped by an excess of small earthquakes, which can be measured by anomalously large b -values.

The idea that magma chambers in the crust may be identified by anomalously high b -values [Wiemer and McNutt, 1997] has been tested on eight volcanoes, so far (section 5). In all cases, relatively small volumes ($0.5 < r < 2$ km) of exceedingly high b -values were found, surrounded by crust with normal values (Plate 1). Beneath volcanoes, where modeling of crustal deformation, seismicity rate and other parameters suggested the presence of magma chambers in specific locations, the b -value anomalies agreed closely with these models (Mount St. Helens, Redoubt, Off-Ito, Long Valley, Mammoth Mountain, east rift of Kilauea). Thus, we believe that the mapping of b -value anomalies beneath volcanoes is an effective tool for locating active magma chambers.

The possible existence of large magma chambers at the base of the crust, or in the upper mantle, can probably not be detected by our method in most cases because the surrounding volumes are not brittle enough to generate earthquakes. In one case, where earthquakes are generated at sub-crustal depths beneath volcanoes, the b -values were anomalously high, identifying a magma reservoir or magma path (Plate 3B). In three of the eight cases, we found two anomalies at different depths (Mount St. Helens, Mammoth Mountain and Aetna), supporting the results of other techniques, which indicated complex magma supply systems.

We favor the interpretation that elevated pore pressures cause the high b -value anomalies beneath volcanoes because an intrusion under Mammoth Mountain changed the b -values at several kilometers distance within less than one month [Wiemer *et al.*, 1998]. We conclude that long-term monitoring of the seismicity of active volcanoes, down to small mag-

nitudes, furnishes important information on the depth, location, size and relative activity of magma chambers and magma supply paths.

9.2. Hypothesis II: *Asperities may be mapped by maxima in local earthquake probability (minima in local recurrence time).*

This hypothesis assumes that the frequency magnitude relationship defined by small earthquakes can be extrapolated to large ones. It is likely that this is not valid for all seismogenic volumes. Nevertheless, the support for the hypothesis, accumulated so far, is strong.

(a) The asperity we mapped under Middle Mountain correlates exactly with the definition of the asperity by other means [Wiemer and Wyss, 1997]. In addition, out of 12 main shocks (San Jacinto-Elsinore plus Kanto-Tokai) 10 correlate with P_L maxima (T_L minima) covering only 10% to 15% of the studied area [Wyss *et al.*, 2000; Wyss and Matsumura, 2001]. The probability that this result was achieved by chance is small.

(b) The values of the recurrence times calculated at Parkfield [Wiemer and Wyss, 1997], along the San Jacinto-Elsinore faults [Wyss *et al.*, 2000], and along the Mexican subduction zone [Zuniga and Wyss, 2001] agree closely with recurrence times estimated based on historically recorded main shocks.

(c) A location close to the epicenter of the 1999 Izmit $M7.4$ main shock was identified in 1998 as the most likely place, along the segment of the North Anatolian fault covered by the German-Turkish seismograph network, to generate a major to large earthquake [Westerhaus *et al.*, 2001].

Thus, we conclude that our method to map asperities promises to be useful in identifying locations that may become crucial in future large earthquakes. In fact, it has already drawn attention to a part of the Mexican subduction zone where the frequent occurrence of $M>7$ events had not been noticed and discussed appropriately.

9.3. Hypothesis III: *The permanent changes in the probability for earthquakes caused by major and large shocks in their vicinity can be estimated from the changes in local recurrence time, calculated from changes in a - and b -values.*

Short-term changes in seismicity due to redistribution of stress has been documented for many main shocks, but in most detail for the Landers 1992 earthquake [Gomberg and Davis, 1996; Harris and Simpson, 1992; Hill *et al.*, 1995; Stein *et al.*, 1992]. This main shock also caused long-term changes in the background seismicity rates and b -values, lasting for many years, which implies that the probability for small and large earthquakes has been changed ‘permanently’ [Wyss and Wiemer, 2000]. By ‘permanent’ we mean duration compa-

rable to the catalog length available since the event. Using equation 7, we estimate that the local probability for a main shock changed by a couple of orders of magnitude in a positive and negative sense in neighboring volumes, respectively (Plate 2E).

We suggest that most main shocks change the probability for future earthquakes permanently in their vicinity, due to changes in the Coulomb fracture criterion [Harris, 1998], and we propose that this may be measured quantitatively by the change in local earthquake probability, extrapolated from the frequency-magnitude distribution. This information can be translated into time-dependent hazard assessment.

9.4. Hypothesis IV: Phase transitions, and thus the deep source of magma for subduction volcanism, may be mapped by anomalously high b -values.

Wiemer and Benoit [1996] formulated this hypothesis, based on their observation that anomalously high b -values were located beneath the volcanoes of the Alaskan and New Zealand subduction zones at the top of the deep seismic zone (100 km depth). In northeastern Japan, we found the same type of anomaly at about 150 km depth, considerably west of the volcanic front [Wyss *et al.*, 2001a]. In the case of northeastern Japan, detailed tomography shows that a low-velocity channel connects this anomaly with the arc volcanoes. Thus, we propose that anomalously high b -values in the depth range of 70 to 160 km at the top of deep earthquake zones may map the origin of fluids for arc magmatism, but that the geometrical relationship between these anomalies and the volcanoes may be complex and depend on yet unknown factors, including the back-flow velocity in the mantle wedge above the descending slab.

9.5. Hypothesis V: The b -values in aftershock sequences are heterogeneous, suggesting that the probability of a major aftershock varies in space.

We have documented that the spatial variability of the a -, p -, and b -values within aftershock sequences is considerable [Wiemer and Katsumata, 1999] and we hypothesize that this information can be effectively translated into probabilistic hazard maps [Wiemer, 2000; Wiemer *et al.*, 2001]. In this model, aftershock hazard, as well as the hazard that an earthquake is followed by an even larger main shock, varies spatially. Particularly, after a large main shock we propose that the hazard at one end of the fault may be quite different from the hazard at the other end. The ultimate aim is to forecast this pattern in near real time after a main shock, based on the first hours and days of aftershock data and an improved understanding of the physical processes causing the asymmetry in aftershocks.

10. Outlook and future work

We anticipate increased interest in the detailed spatial mapping of b -values on a local scale in the next years. The quality and quantity of seismicity catalogs is improving rapidly. The ability to perform precise relocations of hypocenters [Gillard *et al.*, 1996; Hauksson, 2000; Waldhauser and Ellsworth, 2001] is starting to produce highly interesting datasets with hypocenter accuracies better than 500 m. Unfortunately, some of these relocation studies are limited to subsets of catalogs. Because not only small magnitudes are eliminated in these subset selections, alterations of the frequency-magnitude distribution result, and hence some of these relocated data sets are may not be useful for b -value mapping unless the lost events are re-inserted in the catalog with their original hypocenters.

Little progress has been made toward significant improvements in the homogeneity of earthquake catalogs, particularly in magnitudes. Magnitudes will continue to differ between networks. Also, network configurations and data processing approaches will continue to change, often introducing artifacts into earthquake catalogs. The presence of these artifacts, and the general lack of independent verification of seismicity-based studies will likely remain a major challenge for all seismicity studies. Incremental progress through, for example, more widespread use of moment magnitudes, improved artifact recognition techniques, real-time monitoring for artifacts, and improved awareness by network operators is possible.

Increased computer power and enhanced imaging software will make 3-dimensional mapping more feasible. The spherical sampling volumes used in three-dimensional mapping are in many cases the most appropriate approach to b -value mapping and, therefore, particularly suited for hypothesis testing.

Rigorous testing of the hypotheses outlined above will commence over the next years, particularly in the area of asperity mapping, temporal changes, and aftershock hazard. Case studies are the natural first step to build up knowledge and form hypotheses. Because the spatial variability of b has considerable implications for earthquake hazard, it is necessary to move beyond case studies toward statistical tests performed a posteriori as well as in real time. We are currently implementing two hypothesis tests: 1) How do we achieve the best forecast of seismicity: using a constant b -value, or spatially variable b ? 2) Do probabilistic aftershock hazard maps provide a significantly better forecast of aftershock hazard than the conventional aftershock hazard assessment? Other tests will follow; however, in volcanic environments (Plate 1) and the subducting slab (Plate 3B) the case study approach will remain the most widely used.

Acknowledgements

The authors would like to thank S. Husen and M. Baer for valuable comments and suggestions that helped to improve the manuscript. Additionally we thank the various data centers that have made their earthquake catalogs available. This work was supported by NSF by grant number EAR 9902717, and by the Wadati foundation at the University of Alaska, Fairbanks. This paper is contribution number 1197 of the Geophysical Institute, ETHZ.

Figures

Plate 1: Three-dimensional images of the b -value distribution beneath and adjacent to volcanoes. Red colors mark volumes producing disproportionately more small earthquakes than the normal crust (blue to green). (A) Mt. St. Helens, Washington, (B) Mt. Redoubt, Alaska, (C) Mammoth Mountain, California, (D) Mt. Etna, Italy, (E) the South Flank and Kaoiki regions near Kilauea, Hawaii.

Plate 2: Maps of the variability of seismicity parameters. (A) Cross section of the Parkfield segment of the San Andreas fault showing the variation of b -value (top), a -value (middle) and the local recurrence time for an $M6$ main shock, calculated from a and b (bottom). The asperity beneath Middle Mountain, defined by the two largest earthquakes during the observation period (stars) is clearly defined by the T_L -plot. (B) The stability of the b -value pattern along the Parkfield segment of the San Andreas fault is demonstrated by mapping it in cross section for four consecutive periods, each ending at the time indicated as the start of the next one, and the last period ending in Jan. 2000. The contrast between the creeping segment (high b -values) and the asperity exists in all periods. (C) The minimum magnitude of complete reporting in central and northern California varies from $M < 1$ in (between San Francisco and Parkfield and in Long Valley) to $M > 3$ off shore. The inset shows two examples of local frequency magnitude distributions in the locations marked by A and B. (D) The variation of b with depth in southern California measured by the ratio of b above and below 5 km depth. In most areas, b -values decrease with depth (red), but in some the opposite trend is found (blue). Areas with not enough earthquakes in either top or bottom to establish a significant change are shown in gray. (E) From the change of the seismicity parameters due to the Landers $M7.3$ earthquake of 1992 a change in the local probability for major earthquakes is calculated (frame C). The background parameters were estimated from the period 1981-1992.4, the new parameters from 1993-1999.7. The change in the a -value (measured by the standard deviate Z in frame A), together with the change in the b -value (frame B) results in an estimated increase in probability that is largest for the northern part of the source volume of the subsequent $M7.1$ earthquake at Hector Mine (frame C).

Plate 3: Maps of b -value variations on various local scales that can be interpreted to reflect differences in stress level or degree of heterogeneity. (A) Variations of b -values in the after-shock sequences of the $M7.3$ Landers and $M7.1$ Hector Mine earthquakes (red: high b -values ~ 1.5). Black lines indicate the areas ruptured in the two main shocks, triangles mark the epicenter. Low b -values are found outside the actual ruptured areas. (B) Anomalies of high b -values (red) in a cross section of the deep seismic zone and the crust beneath northeastern Japan correlate with the ends of a low V_S velocity channel (gray) in the mantle wedge above the slab, suggesting that material generated at 150 km depth in the upper part of the slab ascends along an inclined path to the arc volcanoes (triangles). Arrows show assumed flow directions. Typically sampling radii are $R=20$ km. (C) Regional b -value map (typically $R=300$ km) of the Himalayas and adjacent areas. Anomalies of high b -values are observed at the two apexes formed by the impact of India on the Asian continent, where stress orientations vary rapidly as a function of space. White lines are based on a numerical model of the stress trajectories. Contrasting frequency magnitude distributions from regions A and B are shown at the right of the map. (D) Maps of the local recurrence time along the San Jacinto fault in southern California, based on small earthquakes recorded during 1981-1999 are compared with the rupture extent of historic main shocks that occurred during 1895-1966. Thick blue lines delineate the extents of ruptures estimated from seismic signal analyses, macroseismic and surface rupture evidence. Circles mark epicenters of after- and foreshocks. The positive correlation suggests that asperities associated with main shocks may be mapped by anomalies in short local recurrence times (blue).

Figure 1: Cumulative frequency of earthquakes in southern California for the years 1995 – 2000 as a function of magnitude. The straight line represents the maximum likelihood estimate of the a - and b -value (equation 1). This estimate is computed based on events above the magnitude of complete recording, $M_c=1.5$.

Figure 2: (A) The maximum likelihood estimate of b as a function of assumed M_c , based on the Parkfield data set from 1980 - 2000. For small M_c , the b -values are systematically underestimated, due to the incompleteness of the catalog. The plateau in the range $1.3 < M_c < 2.5$ indicates that the catalog is complete. The increase in the uncertainty with elevated minimum magnitudes (error bars in Figure 2A) is caused by the decreasing sample size. (B) Range of b -values as a function of sample size. A sample of size N was drawn randomly from a synthetic catalog of 5000 events with a b -value of 1.0. The maximum likelihood and weighted least squares b -value was estimated for this sample, and the process repeated 1000 times. Plotted for each sample size are the 5, 50 and 95 percentiles, illustrating the uncertainty in the

estimate of b . As sample size increases, the uncertainty decreases. The maximum likelihood method gives a less biased and less uncertain estimate than the weighted least squares method.

Figure 3: Explanation of the method used to estimate the minimum magnitude of completeness, M_c . The three frames at the top show synthetic fits to the observed catalog for three different minimum magnitude cutoffs. The bottom frame shows the goodness of fit R , the difference between the observed and a synthetic FMD as a function of lower magnitude cut-off. Numbers correspond to the examples in the top row. The M_c selected is the magnitude at which 90% of the observed data are modeled by a straight line fit.

Figure 4: Example of a magnitude shift, observed in the Tohoku region of Japan. Shown is the non-cumulative FMD, circles mark events recorded in the earlier period (1984.27 – 1987.27), crosses the later period (1988.73 – 1991.09). The shift between the FMD's of the two periods suggests that in 1988 a change occurred in the way magnitudes were reported. This shift was confirmed by a comparison with an independent data set.

Figure 5: (A) Map of central and interior Alaska, gray-shaded is the ratio of daytime to nighttime events, R_q . Dark regions indicate the presence of quarries and mines, active mainly during daytime hours. The data used were provided by the Alaska Earthquake Information Center for the period 1989 – 1998, the sample size was $N=200$ earthquakes. (B, C) Histogram of the hourly distribution (in local time) of the seismicity for two selected regions: An explosion rich volume (1) and a normal volume (2).

Figure 6: Top: NW-SE trending cross-sectional view along the strike of the San Andreas fault of the seismicity in the Parkfield region ($M>1$, 1980 – 2000), dots represent hypocenters. Middle: Nodes used to map the seismicity are plotted as dots. For selected nodes the circle encompassing the $N=100$ nearest hypocenters to that node are plotted. The radii of the circles are inversely proportional to the density of earthquakes, and indicate the local resolution of the method. Bottom: Contour plot of the sampling radii shown above, dark colors indicate a poor spatial resolution.

Figure 7: Comparison of the frequency-magnitude distribution for the creeping part of the San Andreas fault (triangles) and the locked part (squares) for the period 1971 - 1981 (A) and the period 1981 - 1996 (B). In the right frame (C), the forecasts for the period 1996 - 2000.2, assuming that the earthquake-size distribution was stationary for the respective volumes, are plotted as solid lines. The forecasts are based on the observation period 1981 - 1996. The observed seismicity (triangles and squares) matches the forecast closely.

Figure 8: (A) (top) The b values as a function of depth for the Parkfield segment of the San Andreas fault. Each b value was calculated for a depth slice containing 250 earthquakes. Vertical bars are the errors in b ; horizontal bars indicate the depth range sampled. (bottom) Histogram of the number of events in 0.5 km depth bins. (right) Frequency-magnitude distribution for two depth ranges: 0-5 km and 7-15 km. (B) same as Figure 8A, but for the Morgan Hill segment of the Calaveras fault.

Figure 9: Differential b -value cross-section through the Mammoth Mountain area. Compared are the b -values for the periods 1983-1989 and 1989-1990.5. A positive value indicates that the b -value increased in the later period. Contour interval is 0.05. Nodes where the difference in b could not be established at the 99% confidence level are left white.

Figure 10: Differential b value map for the Morgan Hill region, comparing the two periods 1971-1984.3 and 1984.3-1985.3. A star marks the 1984, M6.2 Morgan Hill hypocenter. Only areas where the difference in the b value is significant at the 95% confidence level are shown. Contour lines represent the slip during the main shock in 0.2-m intervals. A positive value of Δb indicates that the b value is higher in the later period. The circle marks the volume of strongest increase in b .

Figure 11: Cumulative (top) and non-cumulative FMD for a shallow volume underneath Mt. Redoubt volcano, Alaska. This volume shows a distinct bi-modal FMD due to the existence of swarm type earthquakes.

References

- Abercrombie, R.E., and J.N. Brune, Evidence for a constant b -value above magnitude 0 in the southern San Andreas, San Jacinto, and San Miguel fault zones and at the Long Valley caldera, California, *Geophys. Res. Lett.*, 21 (15), 1647-1650, 1994.
- Abercrombie, R.E., Earthquake source scaling relationships from -1 to 5 ML using seismograms recorded at 2.5-km depth, *J. Geophys. Res.*, 100, 24014-24036, 1995.
- Aki, K., Maximum likelihood estimate of b in the formula $\log N = a - b M$ and its confidence limits, *Bull. Earthq. Res. Inst.*, 43, 237-239, 1965.
- Aki, K., A probabilistic synthesis of precursory phenomena, in *Earthquake Prediction: An International Review*, edited by D.W. Simpson, and P.G. Richards, pp. 566-574, AGU, Washington, DC, 1981.
- Amelung, F., and G. King, Earthquake scaling laws for creeping and non-creeping faults, *Geophys. Res. Lett.*, 24, 507-510, 1997.
- Bak, P., and C. Tang, Earthquakes as a self-organized critical phenomenon, *J. Geophys. Res.*, 94, 15635-15637, 1989.
- Bakun, W.H., and T.V. McEvilly, Recurrence models and Parkfield, California, earthquakes, *J. Geophys. Res.*, 89, 3051-3058, 1984.

- Barton, D.J., G.R. Foulger, and J.R. Henderson, Frequency-magnitude statistics and spatial correlation dimensions of earthquakes at Long Valley caldera, California, *Geophys. J. Int.*, 129, 138, 563-570, 1999.
- Bender, B., Maximum likelihood estimation of b-values for magnitude grouped data, *Bull. Seism. Soc. Am.*, 73, 831-851, 1983.
- Bowman, D.D., G. Ouillon, C.G. Sammis, A. Sornette, and D. Sornette, An observational test of the critical earthquake concept, *J. Geophys. Res.*, 103, 24359-24372, 1998.
- Byerlee, J., and J.C. Savage, Coloumb plasticity within the fault zone, *Geophys. Res. Letts.*, 19, 2341-2344, 1992.
- De Luca, L., S. Lasocki, D. Luzio, and M. Vitale, Fractal dimension confidence interval estimation of epicentral distributions, *Annal. Geofis.*, 42, 911-925, 1999.
- Frankel, A., Mapping hazard in the central and eastern United States, *Seism. Res. Letts.*, 66, 8-21, 1995.
- Frohlich, C., and S. Davis, Teleseismic b-Values: Or, Much Ado about 1.0, *J. Geophys. Res.*, 98, 631-644, 1993.
- Gerstenberger, M., S. Wiemer, and D. Giardini, A systematic test of the hypothesis that the b value varies with depth in California, *Geoph. Res. Letts.*, 28, 57-60., 2001.
- Gerstenberger, M.C., S. Wiemer, D. Giardini, E. Hauksson, and L.M. Jones (2001b), Time-dependent hazard assessment for California in near real-time, *Seism. Res. Letts.*, 72, 273.
- Gibowicz, S.J., and S. Lasocki, Seismicity induced by mining: Ten years later, *Advances in Geophysics*, Vol. 44, 44, 39-181, 2001.
- Gillard, D., A.M. Rubin, and P. Okubo, Highly concentrated seismicity caused by deformation of Kilauea's deep magma system, *Nature*, 384, 343-346, 1996.
- Gomberg, J., Seismicity and detection/location threshold in the southern Great Basin seismic network, *J. Geophys. Res.*, 96 (B10), 16,401-16,414, 1991.
- Gomberg, J., and S. Davis, Stress/strain changes and triggered seismicity following the Mw7.3 Landers, California, earthquake, *J. Geophys. Res.*, 101, 751-764, 1996.
- Gomberg, J., P. Reasenber, P. Bodin, and R. Harris, Earthquake triggering by transient seismic waves following the Landers and Hector Mine, California earthquakes, *Nature*, 411, 462-466, 2001.
- Gutenberg, B., and C.F. Richter, Magnitude and energy of earthquakes, *Ann. Geofis.*, 9, 1-15, 1954.
- Gutenberg, R., and C.F. Richter, Frequency of earthquakes in California, *Bull. Seism. Soc. Am.*, 34, 185-188, 1944.
- Guttorp, P., On Least-Squares Estimation of B-Values, *Bull. Seism. Soc. Amer.*, 77 (6), 2115-2124, 1987.
- Guttorp, P., and D. Hopkins, On Estimating Varying B-Values, *Bull. Seism. Soc. Amer.*, 76 (3), 889-895, 1986.
- Habermann, R.E., Consistency of teleseismic reporting since 1963, *Bull. Seism. Soc. Am.*, 72, 93-112, 1982.
- Habermann, R.E., Teleseismic detection in the Aleutian Island arc, *J. Geophys. Res.*, 88, 5056-5064, 1983.
- Habermann, R.E., Man-made changes of Seismicity rates, *Bull. Seism. Soc. Am.*, 77, 141-159, 1987.
- Habermann, R.E., and M.S. Craig, Comparison of Berkeley and CALNET magnitude estimates as a means of evaluating temporal consistency of magnitudes in California, *Bull. Seism. Soc. Am.*, 78, 1255-1267, 1988.
- Habermann, R.E., Seismicity rate variations and systematic changes in magnitudes in teleseismic catalogs, *Tectonophysics*, 193, 277-289, 1991.

- Hamilton, R.M., Mean magnitude of an earthquake sequence, *Bull. Seism. Soc. Am.*, 57, 1115-1116, 1967.
- Hardebeck, J.L., J.J. Nazareth, and E. Hauksson, The static stress change triggering model: Constraints from two southern California aftershock sequences, *J. Geophys. Res.-Solid Earth*, 103 (B10), 24427-24437, 1998.
- Harris, R., Introduction to special section: Stress triggers, stress shadows, and implications for seismic hazard, *J. Geophys. Res.*, 103, 24347-24358, 1998.
- Harris, R.A., and R.W. Simpson, Changes in static stress on southern California faults after the 1992 Landers earthquake, *Nature*, 360, 251-254, 1992.
- Harte, D., and D. Vere-Jones, Differences in coverage between the PDE and New Zealand local earthquake catalogues, *N. Z. J. Geol. Geophys.*, 42 (2), 237-253, 1999.
- Hauksson, E., Crustal structure and seismicity distribution adjacent to the Pacific and North America plate boundary in southern California, *J. Geophys. Res.*, 105, 13875-13903, 2000.
- Henderson, J.R., I.G. Main, P.G. Meredith, and P.R. Sammonds, The evolution of seismicity at Parkfield, California - observation, experiment and a fracture-mechanical interpretation, *Journal of Structural Geology*, 14, 905-913, 1992.
- Hill, D.P., M.J.S. Johnston, and J.O. Langbein, Response of Long Valley caldera to the Mw=7.3 Landers, California, earthquake, *J. Geophys. Res.*, 100, 12985-13005, 1995.
- Hirata, T., A correlation of b-value and fractal dimension of earthquakes, *Journal of Geophysical Research*, 94, 7507-7514, 1989.
- Hough, S.E., and L.M. Jones, Aftershocks: Are they earthquakes or afterthoughts?, *Eos, Trans. AGU*, 78, 505, 1997.
- Imoto, M., N. Hurukawa, and Y. Ogata, Three-dimensional spatial variations of b-value in the Kanto area, Japan, *Zishin*, 43, 321-326, 1990.
- Ishimoto, M., and K. Iida, Observations of earthquakes registered with the microseismograph constructed recently, *Bull. Earthq. Res. Inst.*, 17, 443-478, 1939.
- Ito, K., and M. Matsuzaki, Earthquakes as self-organized critical phenomena, *J. Geophys. Res.*, 95, 6853-6860, 1990.
- Jolly, A.D., and S.R. McNutt, Seismicity at the volcanoes of Katmai National Park, Alaska; July 1995-December 1997, *Journal of Volcanology and Geothermal Research*, 93, 173-190, 1999.
- Jones, L.M., and E. Hauksson, The seismic cycle in southern California: Precursor or response?, *Geoph. Res. Letts.*, 24, 469-472, 1997.
- Kagan, Y.Y., Fractal dimension of brittle fracture, *J. Nonlinear Sci.*, 1, 1-16, 1991.
- Kagan, Y.Y., and L. Knopoff, Spatial distribution of earthquakes: The two-point correlation function, *Geophys. J. Roy. Astr. Soc.*, 62, 303-320, 1980.
- Kagan, Y., Universality of the seismic moment-frequency relation, *PAGEOP*, 155, 537-574, 1999.
- Kanamori, H., and D.L. Anderson, Theoretical basis of some empirical relations in seismology, *Bull. Seism. Soc. Am.*, 65, 1073-1095, 1975.
- Kijko, A., and M.A. Sellevoll, Estimation of Earthquake Hazard Parameters from Incomplete Data Files .1. Utilization of Extreme and Complete Catalogs with Different Threshold Magnitudes, *Bull. Seism. Soc. Amer.*, 79 (3), 645-654, 1989.
- Kijko, A., and M.A. Sellevoll, Estimation of Earthquake Hazard Parameters from Incomplete Data Files .2. Incorporation of Magnitude Heterogeneity, *Bull. Seism. Soc. Amer.*, 82 (1), 120-134, 1992.

- King, G.C.P., The accommodation of large strains in the upper lithosphere of the earth and other solids by self-similar fault systems: the geometrical origin of b-value, *PAGEOP*, 121, 761-815, 1983.
- King, G.C.P., R.S. Stein, and J. Lin, Static Stress Changes and the Triggering of Earthquakes, *Bull. Seism. Soc. Am.*, 84 (3), 935-953, 1994.
- Kisslinger, C., and L.M. Jones, Properties of aftershocks in southern California, *J. Geophys. Res.*, 96, 11,947-11,958, 1991.
- Knopoff, L., The magnitude distribution of declustered earthquakes in Southern California, *Proc. Natl. Acad. Sci. U. S. A.*, 97 (22), 11880-11884, 2000.
- Knopoff, L., Y.Y. Kagan, and R. Knopoff, b-values for fore- and aftershocks in real and simulated earthquake sequences, *Bull. Seism. Soc. Am.*, 72, 1663-1676, 1982.
- Knopoff, L., T. Levshina, V.I. Keilis-Borok, and C. Mattoni, Increased long-range intermediate-magnitude earthquake activity prior to strong earthquakes in California, *J. Geophys. Res.*, 101, 5779-5796, 1996.
- Lahaie, F., and J.R. Grasso, Loading rate impact on fracturing pattern: Lessons from hydrocarbon recovery, Lacq gas field, France, *J. Geophys. Res.*, 104, 17941 - 17954, 1999.
- Lockner, D.A., and J.D. Byrlee, Precursory AE patterns leading to rock fracture, in *Proceedings, 5th Conference on Acoustic Emission/Microseismic Activity in Geologic Structures and Materials*, edited by H.R. Hardy, pp. 1-14, Trans-Tech. Publications, Clausthal-Zellerfeld, Germany, 1991.
- Main, I.G., Apparent breaks in scaling in the earthquake cumulative frequency-magnitude distribution: fact or artifact?, *Bull. Seism. Soc. Am.*, 90, 86-97, 2000.
- Main, I.G., Earthquakes as critical phenomena: Implications for probabilistic seismic hazard analysis, *Bull. Seism. Soc. Am.*, 85, 1299-1308, 1995.
- Main, I.G., Statistical physics, seimogenesis, and seismic hazard, *Reviews of Geophysics*, 34 (4), 433-462, 1996.
- Main, I.G., P.G. Meredith, and C. Jones, A Reinterpretation of the Precursory Seismic B-Value Anomaly from Fracture-Mechanics, *Geophysical Journal-Oxford*, 96 (1), 131-138, 1989.
- Miller, S.A., Fluid-mediated influence of adjacent thrusting on the seismic cycle at Parkfield, *Nature*, 382, 799-802, 1996.
- Mogi, K., Magnitude-Frequency Relation for Elastic Shocks Accompanying Fractures of Various Materials and some Related Problems in Earthquakes, *Bull. Earthq. Res. Inst.*, 40, 831-853, 1962.
- Mori, J., and R.E. Abercrombie, Depth dependence of earthquake frequency-magnitude distributions in California: Implications for the rupture initiation, *J. Geophys. Res.*, 102, 15081-15090, 1997.
- Murru, M., C. Montuori, M. Wyss, and E. Privitera, The location of magma chambers at Mt. Etna, Italy, mapped by b-values, *Geoph. Res. Letts.*, 26, 2553-2556, 1999.
- Nadeau, R.M., and T.V. McEvelly, Fault slip rates at depth from recurrence intervals of repeating microearthquakes, *Science*, 285, 718-721, 1999.
- Nadeau, R.M., and L.R. Johnson, Seismological studies at Parkfield VI: Moment release rates and estimates of source parameters for small repeating earthquakes, *Bull. Seism. Soc. Amer.*, 88 (3), 790-814, 1998.
- Narkunskaya, G.S., and M.G. Shnirman, On an algorithm of earthquake prediction, *CSG*, 1, 20-24., 1994.
- Nerenberg, M.A.H., and C. Essex, Correlation dimension and systematic geometric effects, *Phys. Rev. A*, 42, 7065-7074, 1990.
- Nur, A., Role of pore fluids in faulting, *Phil. Trans. R. Soc. Lond. A*, 274, 297-304, 1973.

- Oencel, A.O., and M. Wyss, The major asperity of the 1999 M7.4 Izmit earthquake, defined by the microseismicity of the two decades before it, *Geophys. J. Int.*, 143, 501-506, 2000.
- Ogata, Y., M. Imoto, and K. Katsura, 3-D spatial variation of b-values of magnitude-frequency distribution beneath the Kanto district, Japan, *Geophys. J. Int.*, 104, 135-146, 1991.
- Ogata, Y., and K. Katsura, Analysis of temporal and spatial heterogeneity of magnitude frequency distribution inferred from earthquake catalogues, *Geophys. J. Int.*, 113, 727-738, 1993.
- Okuda, S., T. Ouchi, and T. Terashima, Deviation of Magnitude Frequency-Distribution of Earthquakes from the Gutenberg-Richter Law - Detection of Precursory Anomalies Prior to Large Earthquakes, *Phys. Earth Planet. Inter.*, 73 (3-4), 229-238, 1992.
- Omori, F., On aftershocks, *Report of Imperial Earthquake Investigation Committee*, 2, 103-109, 1894.
- Pacheco, J.F., C.H. Scholz, and L.R. Sykes, Changes in frequency-size relationship from small to large earthquakes, *Nature*, 355, 71-73, 1992.
- Page, R., Aftershocks and microaftershocks of the great Alaska earthquake of 1964, *Bull. Seism. Soc. Am.*, 58, 1131-1168, 1968.
- Papadopoulos, G.A., H.G. Skafida, and I.T. Vassiliou, Nonlinearity of the Magnitude-Frequency Relation in the Hellenic Arc-Trench System and the Characteristic Earthquake Model, *J. Geophys. Res.-Solid Earth*, 98 (B10), 17737-17744, 1993.
- Patane, D., T. Caltabiano, E. Del Pezzo, and S. Gresta, Time variation of b and Qc at Mt. Etna (1981-1987), *Phys. Earth Planet. Interiors*, 71, 137-140, 1992.
- Pechmann, J.C., S.J. Nava, J.C. Bernier, and W.J. Arabasz, A critical analysis of systematic time-dependent coda-magnitude errors in the University of Utah earthquake catalog, 1981-1999, *EOS, Trans. Am. Geophys. Union*, 81, F869, 2000.
- Power, J.A., M. Wyss, and J.L. Latchman, Spatial variations in frequency-magnitude distribution of earthquakes at Soufriere Hills volcano, Montserrat, West Indies, *Geoph. Res. Letts.*, 25, 3653-3656, 1998.
- Rhoades, D.A., Estimation of the Gutenberg-Richter relation allowing for individual earthquake magnitude uncertainties, *Tectonophysics*, 258 (1-4), 71-83, 1996.
- Reasenberg, P.A., Second-order moment of Central California Seismicity, *J. Geophys. Res.*, 90, 5479-5495, 1985.
- Reasenberg, P.A., and L.M. Jones, Earthquake hazard after a mainshock in California, *Science*, 243, 1173-1176, 1989.
- Reasenberg, P.A., and L.M. Jones, California aftershock hazard forecast, *Science*, 247, 345-346, 1990.
- Reasenberg, P.A., and L.M. Jones, Earthquake aftershocks: Update, *Science*, 265, 1251-1252, 1994.
- Rice, J.R., in *Fault mechanics and transport properties*, edited by B. Evans, and T.F. Wong, pp. 475-503, Academic Press, San Diego, CA, 1992.
- Robertson, M.C., C.G. Sammis, M. Sahimi, and A.J. Martin, Fractal analysis of three-dimensional spatial distributions of earthquakes with a percolation interpretation, *J. Geophys. Res.*, 100, 609-620, 1995.
- Rotwain, I., V. Keilis-Borok, and L. Botvina, Premonitory transformation of steel fracturing and seismicity, *Phys. Earth Planet. Int.*, 101, 61-71, 1997.
- Rydelek, P.A., and I.S. Sacks, Testing the completeness of earthquake catalogs and the hypothesis of self-similarity, *Nature*, 337, 251-253, 1989.
- Sammis, C., M. Wyss, R. Nadeau, and S. Wiemer, Comparison between seismicity on creeping and locked patches of the San Andreas fault near Parkfield, California: fractal dimension and b-value, *Bull. Seism. Soc. Am.*, submitted, 2001.
- Scholz, C.H., The Frequency-Magnitude Relation of Microfracturing in Rock and its Relation to Earthquakes, *Bull. Seism. Soc. Am.*, 58, 399-415, 1968.

- Schwartz, D.P., and K.J. Coppersmith, Fault behaviour and characteristic earthquakes: Examples from the Wasatch and San Andreas fault zones, *J. Geophys. Res.*, 89, 5681-5698, 1984.
- Shaw, B.E., Frictional weakening and slip complexity in earthquake faults, *J. Geophys. Res.*, 100, 18239-18252, 1995.
- Shi, Y., and B.A. Bolt, The standard error of the Magnitude-frequency b value, *Bull. Seism. Soc. Am.*, 72, 1677-1687, 1982.
- Smith, W.D., Evidence for Precursory Changes in the Frequency Magnitude B- Value, *Geophys. J. R. Astron. Soc.*, 86 (3), 815-838, 1986.
- Smith, W.D., Predicting Earthquakes in New-Zealand, *Search*, 21 (7), 223-226, 1990.
- Smith, W.D., Resolution and significance assessment of precursory changes in mean earthquake magnitudes, *Geophys. J. Int.*, 135 (2), 515-522, 1998.
- Stein, R.S., G.C.P. King, and J. Lin, Change in failure stress on the San Andreas and surrounding faults caused by the 1992 M=7.4 Landers earthquake, *Science*, 258, 1328-1332, 1992.
- Stein, R.S., and T.C. Hanks, M \geq 6 earthquakes in southern California during the twentieth century: No evidence for a seismicity or moment deficit, *Bull. Seism. Soc. Am.*, 88, 635-652, 1998.
- Tinti, S., Bayesian Interval Estimation of the Parameter B for Grouped Magnitudes, *Tectonophysics*, 168 (4), 319-326, 1989.
- Tinti, S., and F. Mulargia, Confidence-Intervals of B-Values for Grouped Magnitudes, *Bull. Seism. Soc. Amer.*, 77 (6), 2125-2134, 1987.
- Trifu, C.I., T.I. Urbancic, and R.P. Young, Source Parameters of Mining-Induced Seismic Events - an Evaluation of Homogeneous and Inhomogeneous Faulting Models for Assessing Damage Potential, *Pure Appl. Geophys.*, 145 (1), 3-27, 1995.
- Turcotte, D.L., *Fractals and chaos in geology and geophysics*, 221 pp., Cambridge University Press, Cambridge, 1992.
- Urbancic, T.I., C.I. Trifu, J.M. Long, and R.P. Young, Space-time correlations of b-values with stress release, *PAGEOP*, 139, 449-462, 1992.
- Utsu, T., A method for determining the value of b in a formula $\log n = a - bM$ showing the magnitude frequency for earthquakes, *Geophys. Bull. Hokkaido Univ.*, 13, 99-103, 1965.
- Utsu, T., On seismicity, in *Report of the Joint Research Institute for Statistical Mathematics*, pp. 139-157, Institute for Statistical Mathematics, Tokyo, 1992.
- Utsu, T., Y. Ogata, and R.S. Matsu'ura, The centenary of the Omori formula for a decay law of after-shock activity, *J. Phys. Earth*, 43, 1-33, 1995.
- Utsu, T., Representation and analysis of the earthquake size distribution: a historical review and some new approaches, *PAGEOP*, 155, 509-535, 1999.
- Varnes, D.J., Predicting earthquakes by analyzing accelerating precursory seismic activity, *PAGEOP*, 130, 661-686, 1989.
- Volant, P., and J.R. Grasso, The finite extension of fractal geometry and power law distribution, *J. Geophys. Res.*, 99, 21,879 - 21,890, 1994.
- Waldhauser, F., and W.L. Ellsworth, A Double-Difference Earthquake Location Algorithm: Method and Application to the Northern Hayward Fault, California, *Bull. Seism. Soc. Am.*, recent, 2001.
- Warren, N.W., and G.V. Latham, An Experimental Study of Thermally Induced Microfracturing and its Relation to Volcanic Seismicity, *J. Geophys. Res.*, 75, 4455-4464, 1970.
- Wesnousky, S.G., The Gutenberg-Richter or characteristic earthquake distribution, which is it?, *Bull. Seism. Soc. Am.*, 84, 1940-1959, 1994.

- Westerhaus, M., M. Wyss, R. Yilmaz, and J. Zschau, Correlating variations of b values and crustal deformations during the 1990s may have pinpointed the rupture initiation of the Mw=7.4 Izmit earthquake of Aug. 17, 1999, *Geophys. J. Int.*, in press, 2001.
- Wiemer, S., and M. Wyss, Seismic quiescence before the Landers (M=7.5) and Big Bear (M=6.5) 1992 earthquakes, *Bull. Seism. Soc. Am.*, *84*, 900-916, 1994.
- Wiemer, S., and J. Benoit, Mapping the b-value anomaly at 100 km depth in the Alaska and New Zealand subduction zones, *Geoph. Res. Letts.*, *23*, 1557-1560, 1996.
- Wiemer, S., and S. McNutt, Variations in frequency-magnitude distribution with depth in two volcanic areas: Mount St. Helens, Washington, and Mt. Spurr, Alaska, *Geoph. Res. Letts.*, *24*, 189-192, 1997.
- Wiemer, S., and M. Wyss, Mapping the frequency-magnitude distribution in asperities: An improved technique to calculate recurrence times?, *J. Geophys. Res.*, *102*, 15115-15128, 1997.
- Wiemer, S., S.R. McNutt, and M. Wyss, Temporal and three-dimensional spatial analysis of the frequency-magnitude distribution near Long Valley caldera, California, *Geophys. J. Int.*, *134*, 409 - 421, 1998.
- Wiemer, S., and K. Katsumata, Spatial variability of seismicity parameters in aftershock zones, *J. Geophys. Res.*, *104*, 13,135-13,151, 1999.
- Wiemer, S., Introducing probabilistic aftershock hazard mapping, *Geoph. Res. Letts.*, *27*, 3405-3408, 2000.
- Wiemer, S., and M. Wyss, Minimum magnitude of completeness in earthquake catalogs: Examples from Alaska, the western US and Japan, *Bull. Seism. Soc. Am.*, *90*, 859-869, 2000.
- Wiemer, S., A software package to analyze seismicity: ZMAP, *Seism. Res. Letts.*, *72*, 373-382, 2001.
- Wiemer, S., M.C. Gerstenberger, and E. Hauksson, Properties of the 1999, Mw7.1, Hector Mine earthquake: Implications for aftershock hazard, *Bull. Seism. Soc. Am.*, in press, 2001.
- Wyss, M., Towards a physical understanding of the earthquake frequency distribution, *Geophysical Journal of the Royal Astronomical Society*, *31*, 341-359, 1973.
- Wyss, M., and W.H.K. Lee, Time variations of the average earthquake magnitude in Central California, in *Proceedings of the Conference on Tectonic Problems of the San Andreas Fault System*, edited by R.L. Kovach, and A. Nur, pp. 24-42, Stanford University Geol. Sci., 1973.
- Wyss, M., Reporting history of the central Aleutians Seismograph network and the quiescence preceding the 1986 Andreanof Island earthquake, *Bull. Seism. Soc. Am.*, *81*, 1231-1254, 1991.
- Wyss, M., K. Shimazaki, and S. Wiemer, Mapping active magma chambers by b-value beneath the off-Ito volcano, Japan, *J. Geophys. Res.*, *102*, 20413-20422, 1997.
- Wyss, M., and S. Wiemer, Two current seismic quiescences within 40 km of Tokyo, *Geophys. J. Int.*, *128*, 459-473, 1997.
- Wyss, M., D. Schorlemmer, and S. Wiemer, Mapping asperities by minima of local recurrence time: The San Jacinto-Elsinore fault zones, *J. Geophys. Res.*, *105*, 7829-7844, 2000.
- Wyss, M., and Y. Toya, Is the Background Seismicity Produced at a Stationary Poissonian Rate?, *Bull. Seism. Soc. Am.*, *90*, 1174-1187, 2000.
- Wyss, M., and S. Wiemer, Change in the probabilities for earthquakes in Southern California due to the Landers M7.3 earthquake, *Science*, *290*, 1334-1338, 2000.
- Wyss, M., A. Hasegawa, and J. Nakajima, Source and path of magma for volcanoes in the subduction zone of northeastern Japan, *Geoph. Res. Letts.*, in press, 2001a.
- Wyss, M., K. Nagamine, F.W. Klein, and S. Wiemer, Evidence for magma at intermediate crustal depth below Kilauea's East Rift, Hawaii, based on anomalously high b-values, *J. Volc. Geoth. Res.*, *106*, 23-37, 2001b.

- Wyss, M., and S. Matsumura, Most likely locations of large earthquakes in the Kanto and Tokai areas, Japan, estimated based on local recurrence time, *Physics of the Earth and Planetary Interiors*, submitted, 2001c.
- Wyss, M., S. Wiemer, and S. Tsuboi, Mapping b-value anomalies in the subducting slabs beneath Japan, using the JUNEC data, *Bull. Seism. Soc. Am.*, submitted, 2001c.
- Zobin, V.M., Variations of volcanic earthquake source parameters before volcanic eruptions, *J. Volcanol. Geotherm. Res.*, 6, 279-293, 1979.
- Zuniga, F.R., and S. Wiemer, Seismicity patterns: are they always related to natural causes?, *PAGEOP*, 155, 713-726, 1999.
- Zuniga, F.R., and M. Wyss, Most and least likely locations of large to great earthquakes along the Pacific coast of Mexico, estimated from local recurrence times based on b-values, *Bull. Seism. Soc. Am.*, 90, in press, 2001.
- Zuniga, R., and M. Wyss, Inadvertent changes in magnitude reported in earthquake catalogs: Influence on b-value estimates, *Bull. Seism. Soc. Am.*, 85, 1858-1866, 1995.

Appendix: Frequently Asked Questions

A.1. Should one use samples with constant numbers, rather than constant radius?

Either approach is equally valid, and often it is a good idea to compare the results of both to make sure that they are independent of the choice of sampling method. By sampling a constant number of events at each node, the sample size, and hence uncertainty, is approximately constant, and the best spatial resolution possible at each node is achieved. In this case, the radii of sampling volumes, or resolution, are inversely proportional to the local density of earthquakes and consequently variable across a region. When using constant radii for sampling, the resolution does not vary spatially, but the sample size, and hence the uncertainty, does. It is necessary to exclude nodes where fewer than a minimum number of earthquakes are sampled (e.g., 50), or one can use a cutoff, based on a maximum for the allowed uncertainty. Recurrence time and probability maps, calculated by equation 6 and 7, require sampling by constant radius, because otherwise the a -value is meaningless.

A.2 Why do we map b -values, not mean magnitude?

The parameter we are interested in is the mean magnitude and not the b -slope. These two parameters are equivalent, because they are inversely proportional to each other (equations 3). Discussions of the b -value can be understood better because the values of b have (or should have) the same meaning in all regional networks, regardless of the magnitude range used to define b . Thus, a value of $b=1.5$ beneath a volcano estimated from earthquakes in the range $0 < M_D < 2.0$ contained in a local catalog, may be judged as anomalously high compared to $b=1$, defined by a regional catalog with events in the range $1.5 < M_D < 5.0$, or even b -values derived from a world-wide catalog in the range of $4.5 < m < 6.5$. On the other hand, the mean magnitude in the three catalogs is different, because it depends on M_c resolved by the network (equation 3). Therefore, comparing mean magnitudes derived from different data sets would be confusing, whereas a discussion of the same property in terms of b -value is informative and understandable.

A.3 Should the catalog be declustered?

Declustering is the separation of the dependent events (i.e., foreshocks, aftershocks and clusters) from the background seismicity [Reasenberg, 1985]. For seismicity rate studies [Wiemer and Wyss, 1994; Wyss and Wiemer, 1997] as well as hazard related studies [Frankel, 1995] declustering is often considered necessary to achieve the best results. When studying aftershock distributions or aftershock hazard [Wiemer and Katsumata, 1999; Wiemer, 2000; Wiemer et al., 2001], the data are not declustered. In the absence of larger aftershock se-

quences in a data set, the impact of declustering generally tends to be small, and it may be advisable to compare the results with and without declustering. In summary, the question of whether or not to decluster a data set prior to analysis cannot be answered universally, as it depends on the problem to be addressed.

A.4 What is the influence of location errors?

If the location errors are random and do not depend on magnitude, we can use any size volume for sampling because, on average, events are randomly moved into and out of the volume in which they really belong. If the errors are random, but larger for small events, then a sample biased toward too many small events can be obtained at the edge of a seismically active volume because selectively small ones are thought erroneously to lie outside the true seismogenic volume. Cases in which systematic errors may depend on magnitude are rare, but can exist. For example, small and medium size earthquakes beneath a volcano may be afflicted by systematically different errors, if they are located by a local and regional network, respectively. Thus, artificial *b*-value anomalies, in particular as a function of depth, may appear. In addition, all hypocenters may be shifted systematically, for example in depth. In this case, the mapping would not be biased, but the tectonic interpretation may be biased.

A.5 What software do you use?

The software we use to do most of our analysis is bundled in a package called ZMAP [Wiemer, 2001]. It is written in the Matlab language, and users will need to purchase a Matlab license to operate ZMAP. ZMAP can be obtained via the Internet at <http://www.seismo.ethz/staff/stefan>. Also, a manual, a cookbook, and sample data sets are available for downloading.

Figure 1

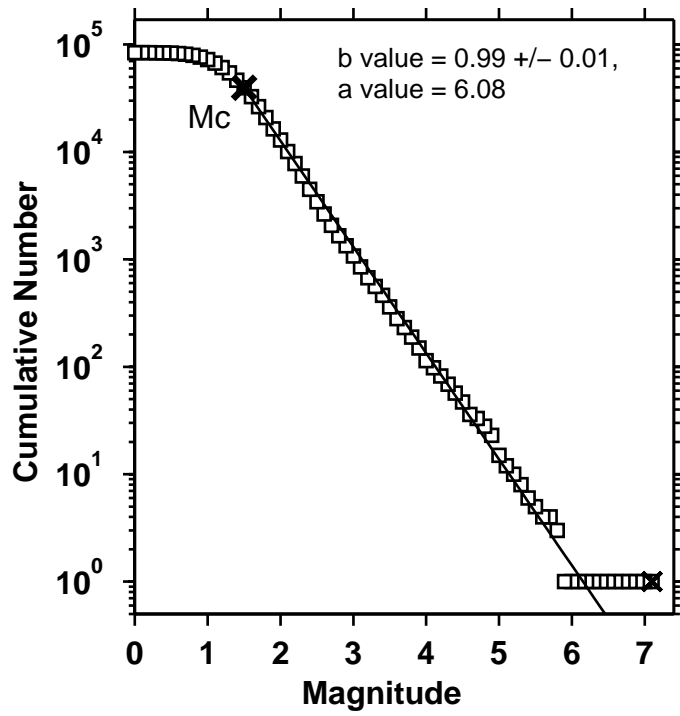


Figure 2

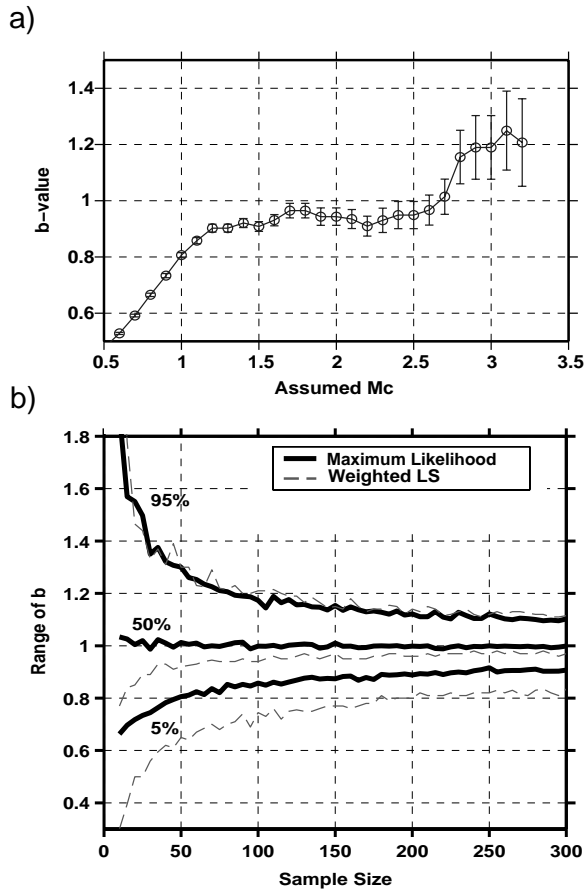


Figure 3

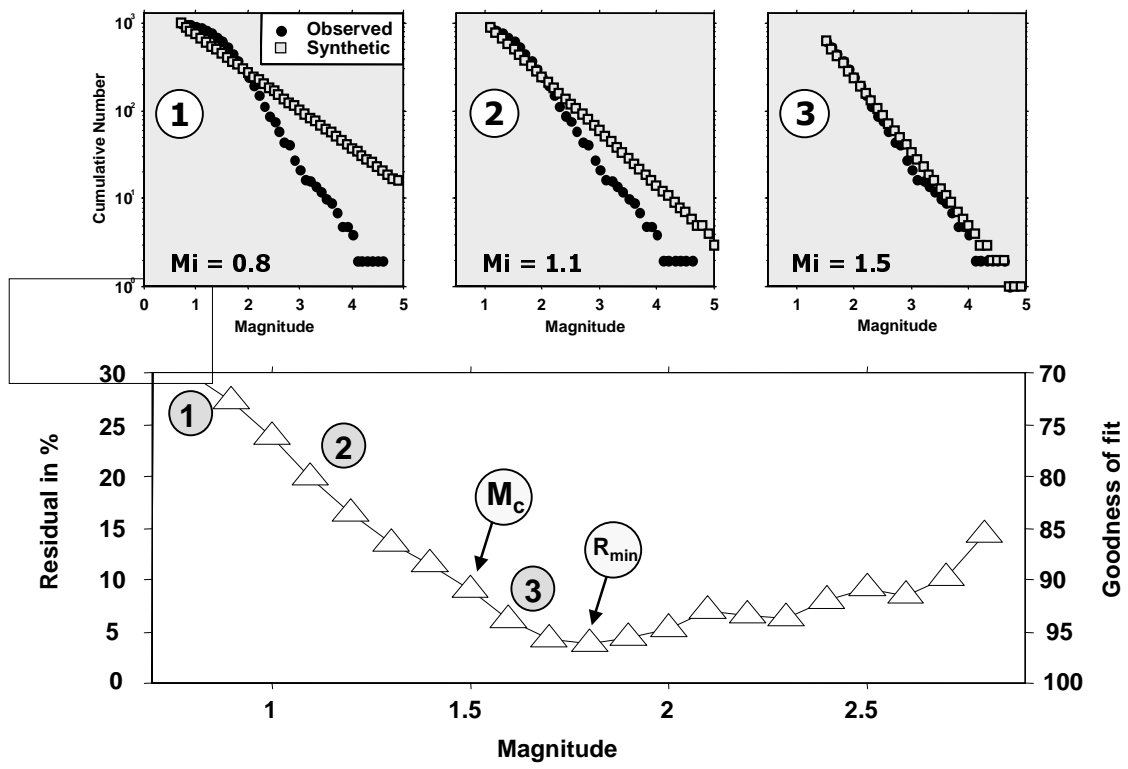


Figure 4

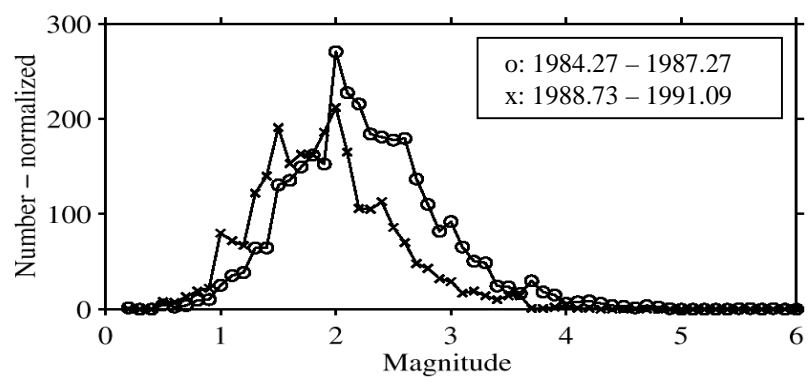
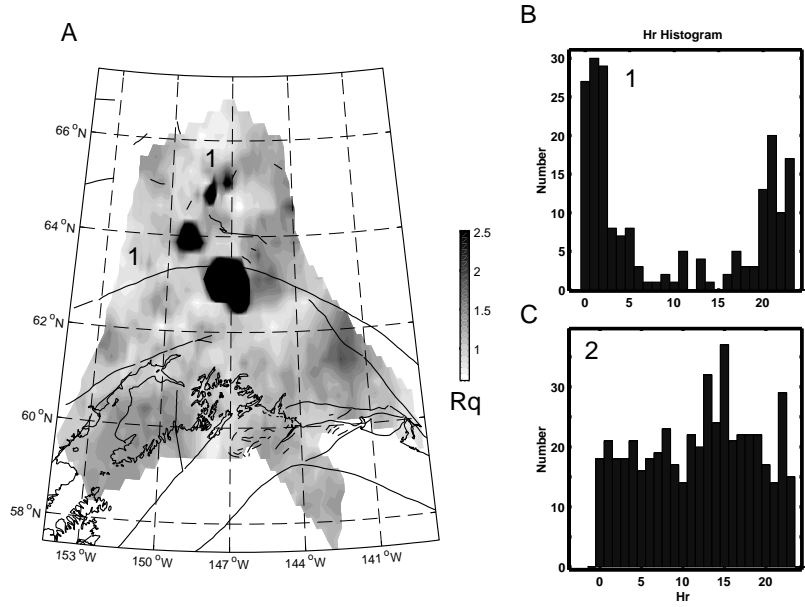


Figure 5



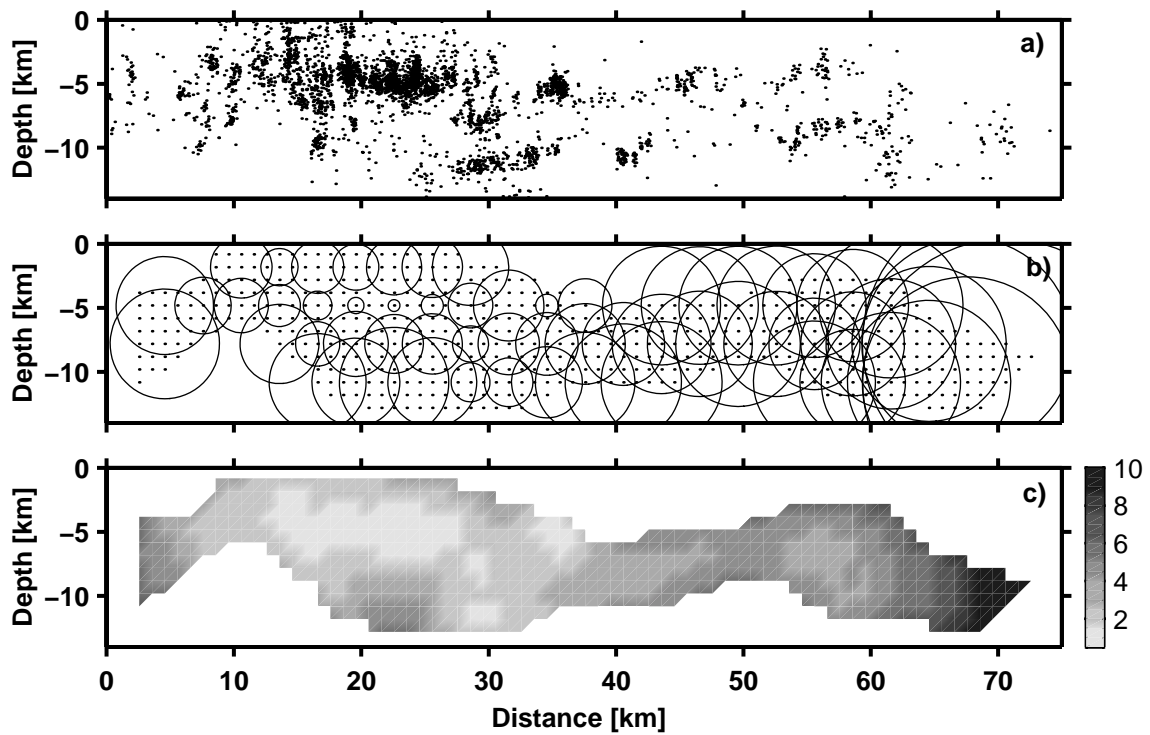


Figure 6

Figure 7

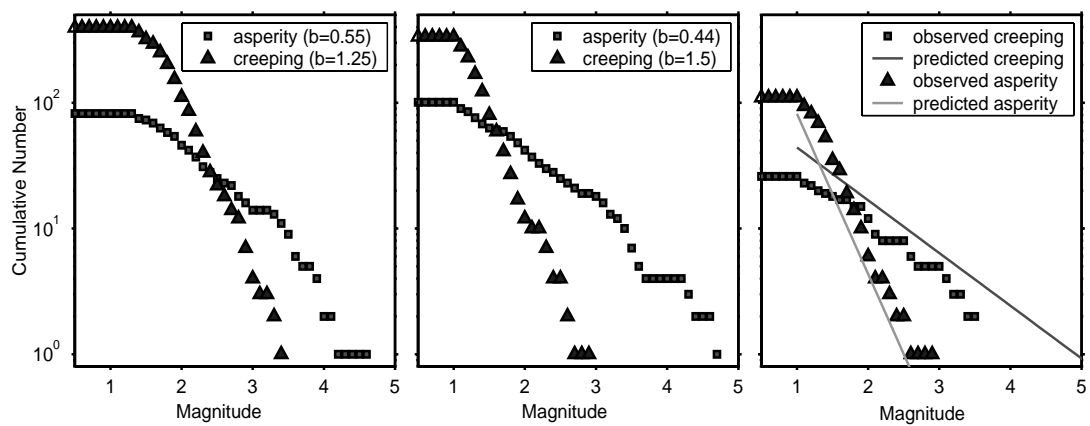
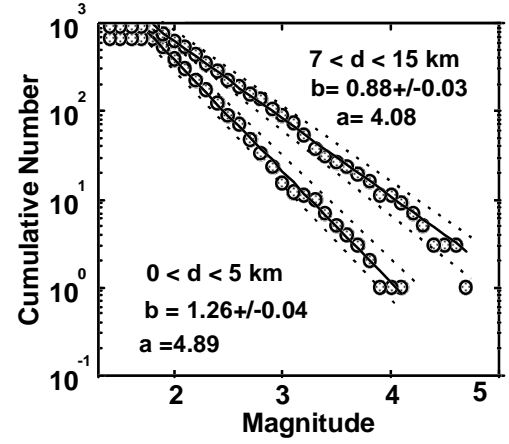
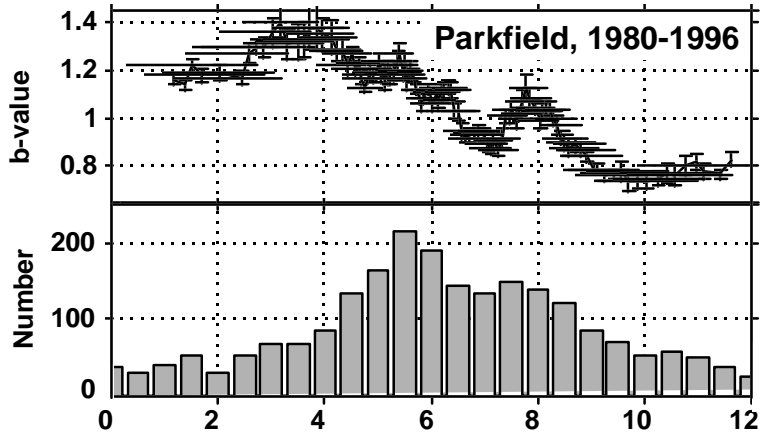


Figure 8

A



B

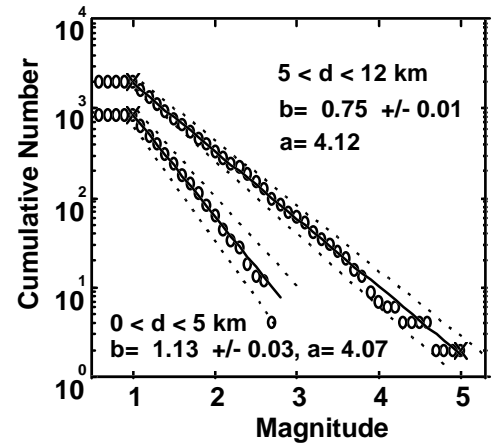
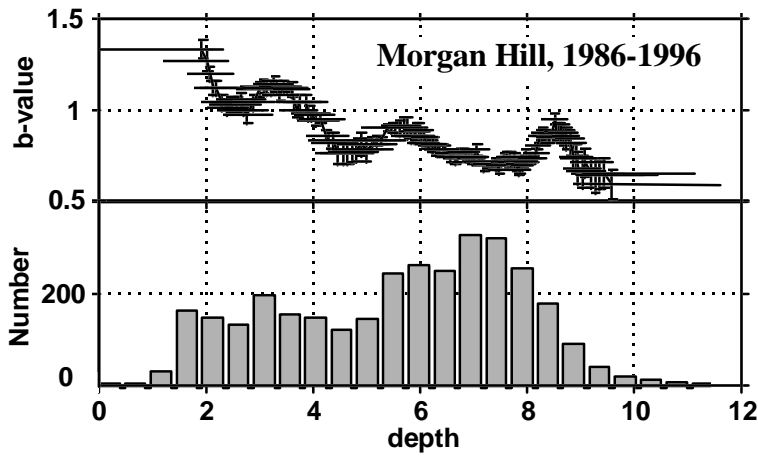


Figure 9

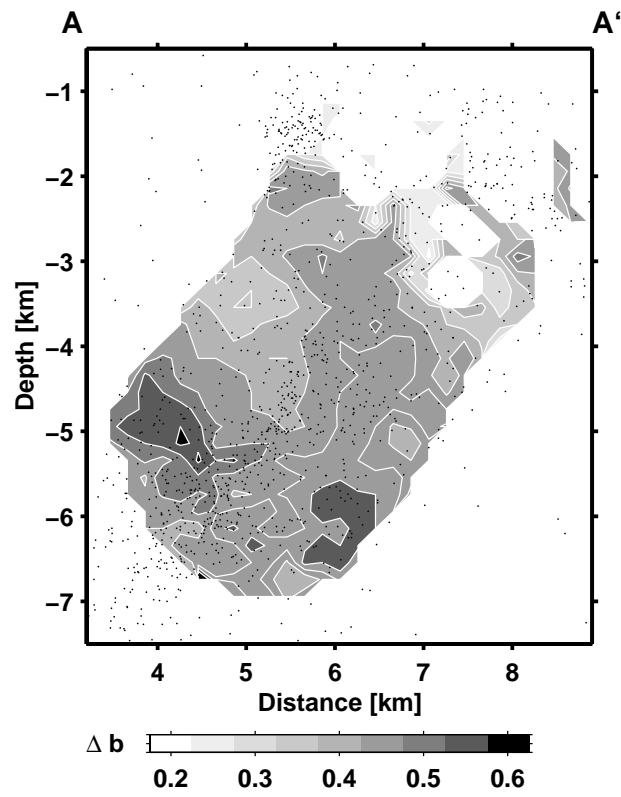


Figure 10

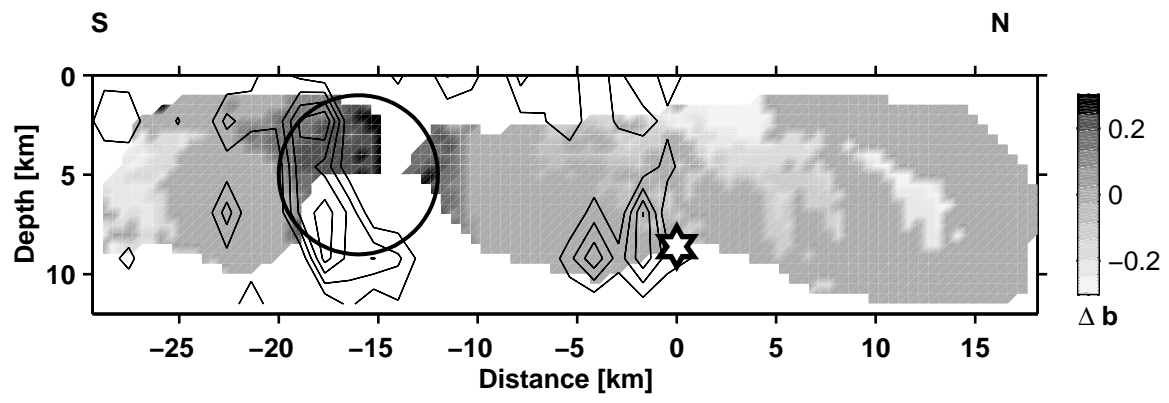
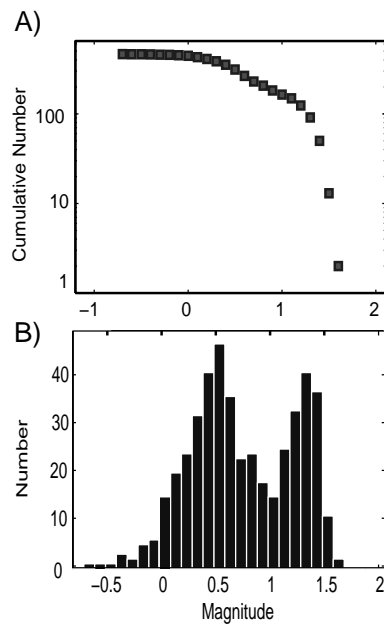
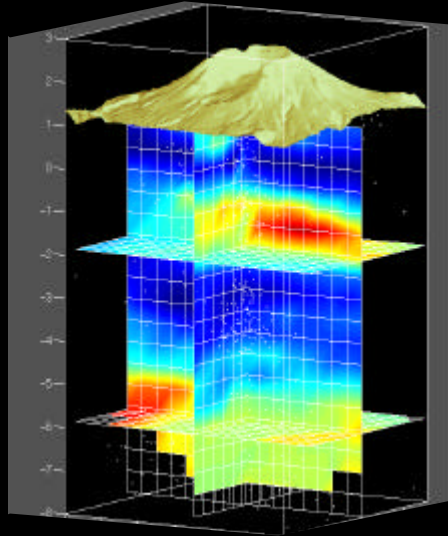


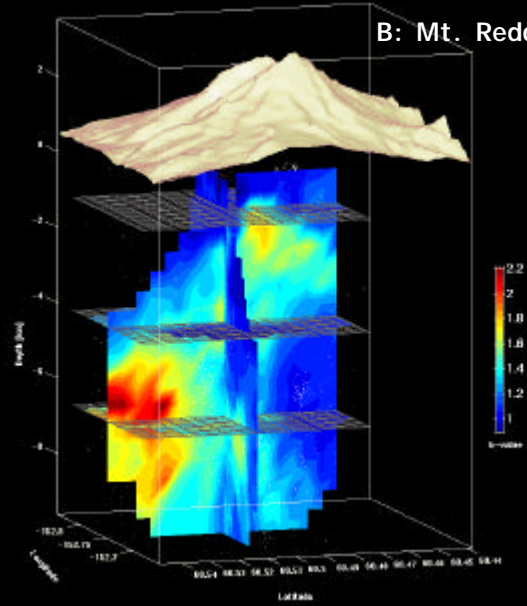
Figure 11



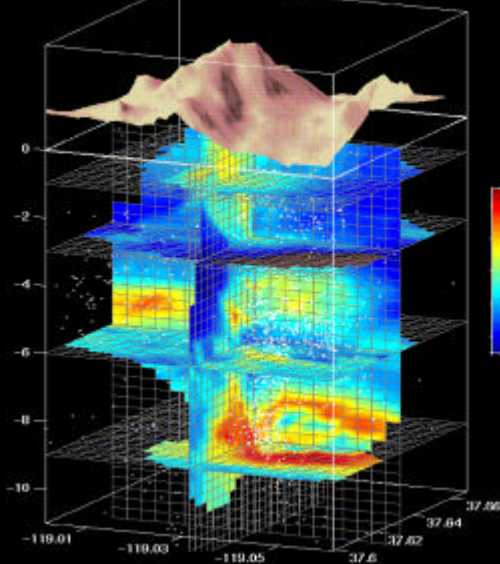
A: Mt. St. Helens



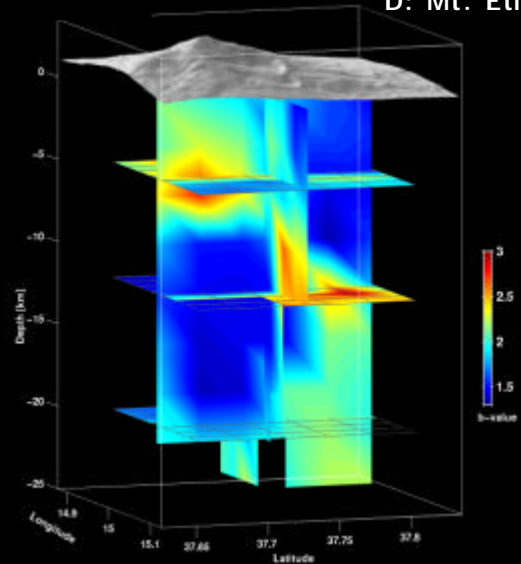
B: Mt. Redoubt



C: Mammoth Mountain



D: Mt. Etna



E: Hawaii

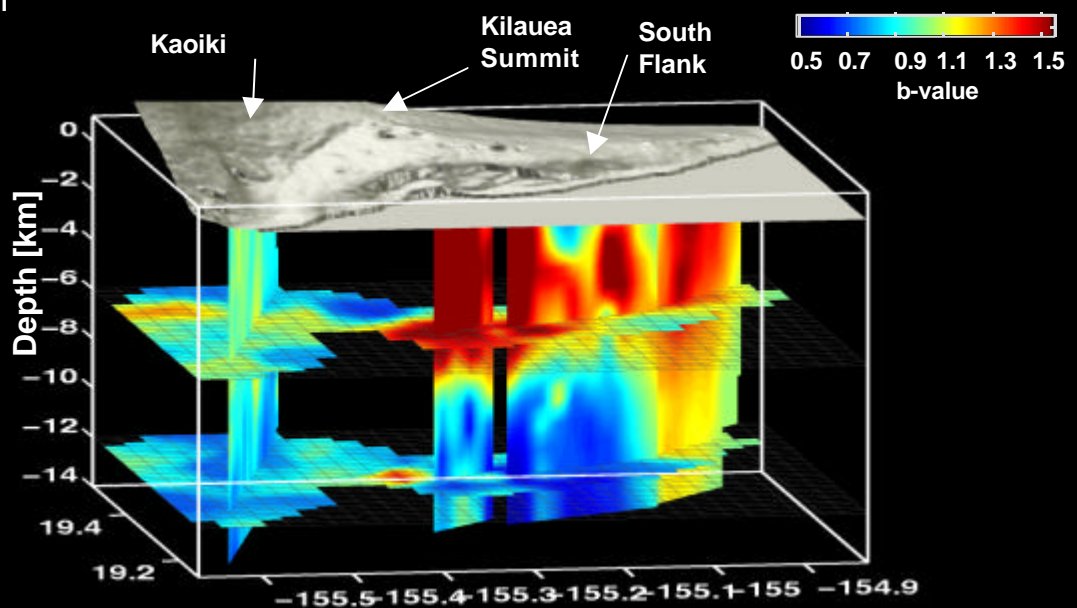


Plate 2

